



Review

Marine Geohazards of the Bay of Naples (Southern Tyrrhenian Sea, Italy): A Review Integrating Morpho-Bathymetric and Seismo-Stratigraphic Analysis

Gemma Aiello ^{1,*} and Mauro Caccavale ^{1,2}

¹ Istituto di Scienze Marine (ISMAR), Consiglio Nazionale delle Ricerche (CNR), Sezione Secondaria di Napoli, 80133 Naples, Italy; mauro.caccavale@cnr.it

² Istituto Nazionale di Geofisica e Vulcanologia (INGV), Osservatorio Vesuviano (OV), 80125 Naples, Italy

* Correspondence: gemma.aiello@cnr.it

Abstract: Marine geohazards in the Bay of Naples, an eruptive region during the late Quaternary, have been assessed based on both morpho-bathymetric and seismic data. Previously identified areas of high marine hazard with slide potential (northern Ischia slope, Naples canyons, and Sorrento Peninsula–Capri slope) have been confirmed and integrated through the seismo-stratigraphic analysis of selected seismic sections. We evaluated the occurrence of important fossil submarine landslides in the stratigraphic record. Several kinds of submarine landslides have been individuated through morpho-bathymetric and seismic interpretation, including creeping, debris avalanches, and debris flows, among others, often controlled by volcanic eruptions. Submarine landslides of Naples Bay are primary geohazards in the marine and coastal areas, which has been ascertained with significant volcanic and tsunami hazards involving the gulf. Despite previous studies on these topics, much work is still needed to compile a systematic database of the submarine landslides of the Bay of Naples, representing a future step of this research.

Keywords: submarine landslides; morpho-bathymetry; seismic stratigraphy; marine geohazards; Bay of Naples; Southern Tyrrhenian Sea



Citation: Aiello, G.; Caccavale, M. Marine Geohazards of the Bay of Naples (Southern Tyrrhenian Sea, Italy): A Review Integrating Morpho-Bathymetric and

Seismo-Stratigraphic Analysis. *GeoHazards* **2024**, *5*, 393–414. <https://doi.org/10.3390/geohazards5020021>

Academic Editor: Fabio Vittorio De Blasio

Received: 21 March 2024

Revised: 25 April 2024

Accepted: 8 May 2024

Published: 10 May 2024



Copyright: © 2024 by the authors. Licensee MDPI, Basel, Switzerland. This article is an open access article distributed under the terms and conditions of the Creative Commons Attribution (CC BY) license (<https://creativecommons.org/licenses/by/4.0/>).

1. Introduction

Marine geohazards are a group of underwater phenomena that can pose a threat to humans and the marine environment, with implications for coastal communities and the Blue Economy [1,2]. Forecasting is difficult because the appearance of a marine hazard can be unexpected and infrequent. These hazards are controlled by earthquakes, volcanoes, tsunamis, and submarine mass movements [1,2].

The seabed of the Mediterranean Sea displays evidence of mass movements [1,2]. Rivers from mountains streams cause unstable seabeds. The submarine canyons trigger submarine landslides over the bottom of the Mediterranean Sea [3–9]. Geological processes associated with plate boundaries and active faulting cause marine hazardous events in the Mediterranean [3]. Steep and unstable continental slopes on the continental margins of the Mediterranean have been controlled by the subduction of the African plate below the Eurasian Plate. Urgeles and Camerlenghi [4] have shown that major deltaic wedges host wide submarine landslides, while tectonically active margins display small failures. Moreover, the available data highlight that submarine landslides are concentrated in the lowstand periods. Ceramicola et al. [5] have shown that the Ionian margins of Calabria and Apulia display four types of mass movements, including the mass transport complexes within intraslope basins, the isolated slide scars along open slopes, the sediment undulations genetically related to fluid migrations, and the headwalls and the sidewall scarps in the submarine canyons. These features represent important geohazards of the Calabria region. Camargo et al. [6] have proposed a review of marine geohazards based

on bibliometric searching. The obtained categories include slope failures, fluid seepages, earthquakes, tsunamis, volcanism, subsidence, bedforms, positive reliefs, negative reliefs, diapirs, faulting, and erosion. Wang and others [8] suggested using offshore bottom pressure gauges (OBPGs) around Crete Island to warn people about tsunamis early by using data assimilation. Heidarzadeh et al. [9] identified the submarine landslide as the trigger of a tsunami observed on February 2023 in the Eastern Mediterranean Sea.

The Bay of Naples, a late Quaternary eruptive region, displays marine geohazards due to volcanism, earthquakes, submarine mass movements, fluid seepages, and anthropogenic impacts. Quaternary volcanism has significantly impacted the sea, controlling the formation of submarine volcanoes, tephra deposits [10–14] (among others), and submarine mass movements [15–18] (among others). Tephra deposits have been detected in southern Naples Bay and northern Salerno Bay, represented in particular by the proximal deposits of the 79 A.D. eruption, along with those of the interplinian activity at 2.7 ka B.P. [12]. These tephra correspond to stratigraphic markers interlayered within the late Holocene marine deposits. Submarine mass movements include creep, debris flows, and debris avalanches. The creeping of Holocene deposits has been recognized at the sea bottom offshore the Sarno pro delta system [10], while debris avalanche deposits have been detected offshore on the southern, northern, and western sides of Ischia [15,16].

Tsunamis in the Bay of Naples have been suggested based on previous results [19–22]. Tinti et al. [19] simulated the tsunami triggered in the Bay of Naples by the pyroclastic flows of the Vesuvius, which entered into the sea and produced an intense pressure pulse. The tsunami was small, but it moved a significant amount of the inside of the bay near Naples and Castellammare [19]. Tinti et al. [20] simulated the tsunami occurring at Ischia Island, as triggered by the Ischia debris avalanche (IDA) [13]. These calculations determined that the eventual tsunami, which was triggered by a debris avalanche having the IDA dimensions, significantly involved the whole Bay of Naples, with the highest waves at Ischia, Capri, and Sorrento Peninsula [20]. Selva et al. [21] analyzed the natural hazards of Ischia, developing their interpretative framework. The obtained results have shown the important role of volcanic hazards (eruptions, tephra), as well as non-volcanic ones (earthquakes, landslides, and tsunamis). Quantitative hazards have still not been evaluated, and the block resurgence of Ischia has a fundamental role in their calculation. Grezio et al. [22] have suggested that the first-order tsunami hazard results have the highest probabilities, exceeding levels of about 1–1.5 m in 50 years, and occur at Naples town, Campi Flegrei, and Ischia.

In this paper, we discuss the marine geohazards of the Bay of Naples, based on both the literature review of the data existing on the area and the morpho-bathymetric and seismic interpretation of marine geohazards, previously identified [23,24] in the northern slope of Ischia, Naples canyons, and southern slope of the Sorrento Peninsula–Capri Island structural elongment. Based on seismic interpretation, we provide further data and constraints on the occurrence of important fossil submarine landslides in Naples Bay, highlighting that different types of submarine landslides can be detected in this complex volcanic area. Figure 1 shows the geologic sketch map of the Bay of Naples and the surrounding emerged areas, while Figure 2 displays a digital elevation model of Naples Bay, with the location of the three study areas, indicated as the sectors having a high marine hazard in Naples Bay [23,24].

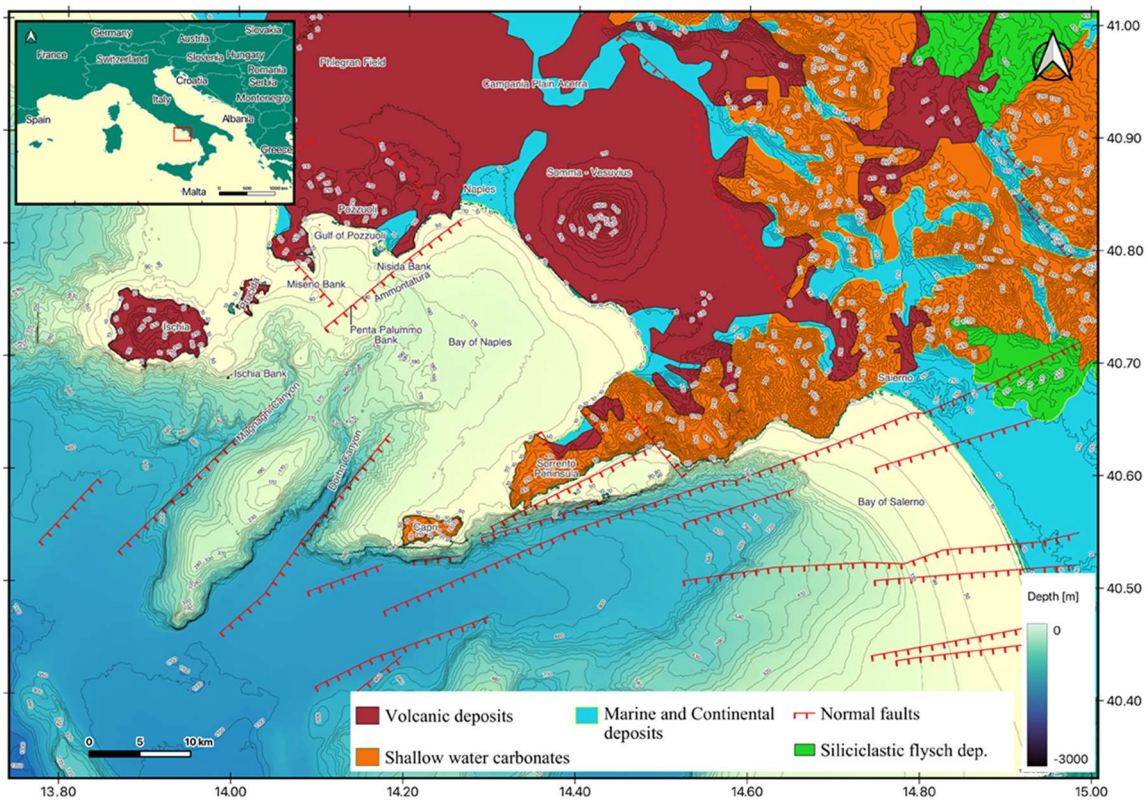


Figure 1. Geologic sketch map of the Bay of Naples and the surrounding emerged areas.

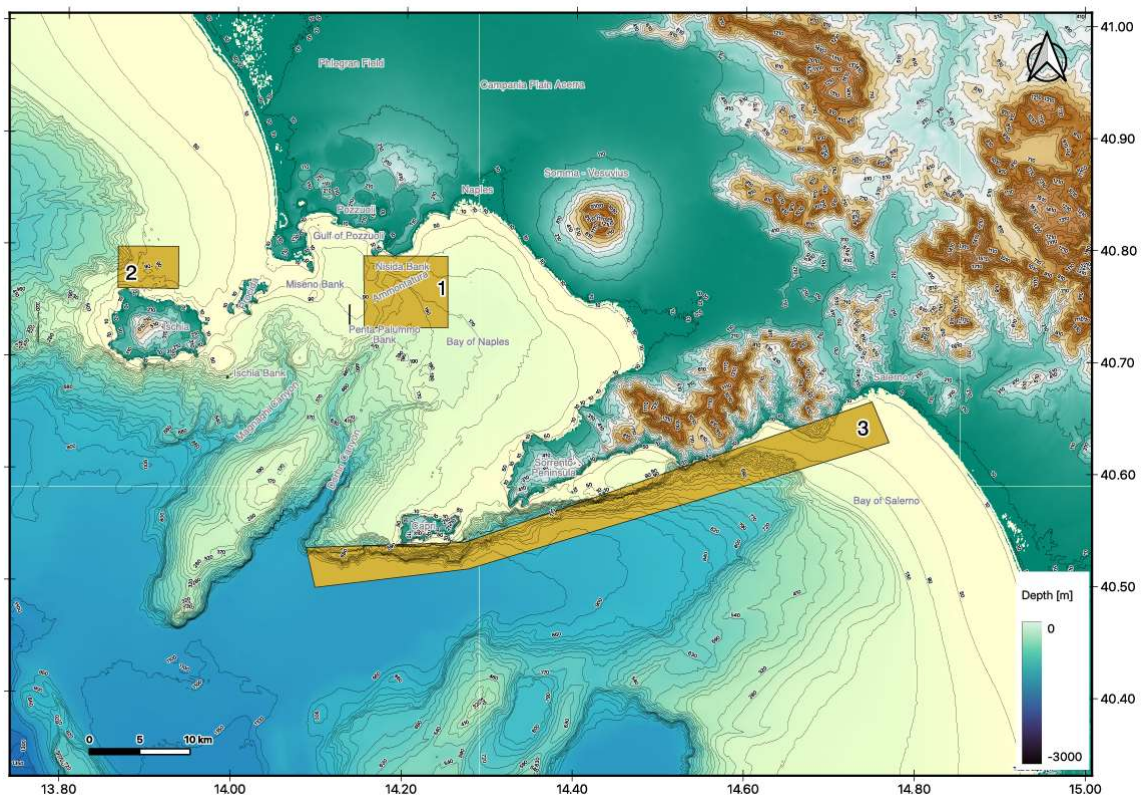


Figure 2. Digital elevation model of Naples Bay showing the location of study areas (1: Ammontatura slope basin and the northern branch of the Dohrn canyon; 2: northern Ischia debris avalanche deposits; 3: southern slope of the Sorrento Peninsula).

2. Geological Setting

The Bay of Naples represents a half-graben on the continental margin, produced by broad extension alongside the Apenninic chain [25] (Figure 1). The geological framework of this basin is characterized by alternating structural highs and lows in a transtensional tectonic setting [26–28]. In the Campania country, Quaternary basin deposits overlie the westerly Apenninic tectono-stratigraphic sequences, arising from the continuation toward the offshore of the matching units outcropping in the marginal zone of the southern Apennines [29,30]. These tectonic assemblages compose the basement of the littoral basins and consist of flysch deposits or of Meso–Cenozoic carbonates (Figure 1).

A structural high with a WSW–ENE trend is found on the Sorrento Peninsula, sandwiched between two half-grabens, the Bay of Naples, and the Bay of Salerno (Figure 1) [31]. Its structural framework is characterized by NW dipping blocks, resulting from tectonic phases ranging in age from the late Miocene to the Quaternary [31].

Mesozoic carbonates appear in the peninsula and are overlain by a transgressive Miocene sequence and then by breccias and pyroclastic rocks that are Pleistocene to Holocene in age (Figure 1). The 79 A.D. pyroclastic unit overlies the Mesozoic rocks or eruptive units of the middle-late Pleistocene. Between 18 ky ago and 79 A.D., the headland did not display appreciable pyroclastic deposits because, during this time frame, the Plinian eruptions were propagated toward the east and northeast [31,32].

Ischia Island has been deeply studied regarding the debris avalanche deposits, both offshore [33–37] and onshore (Figure 3a [37]). Seven debris avalanches surround the Epomeo Mt., showing a close relationship with the corresponding deposits on the continental shelf [38] (Figure 3b).

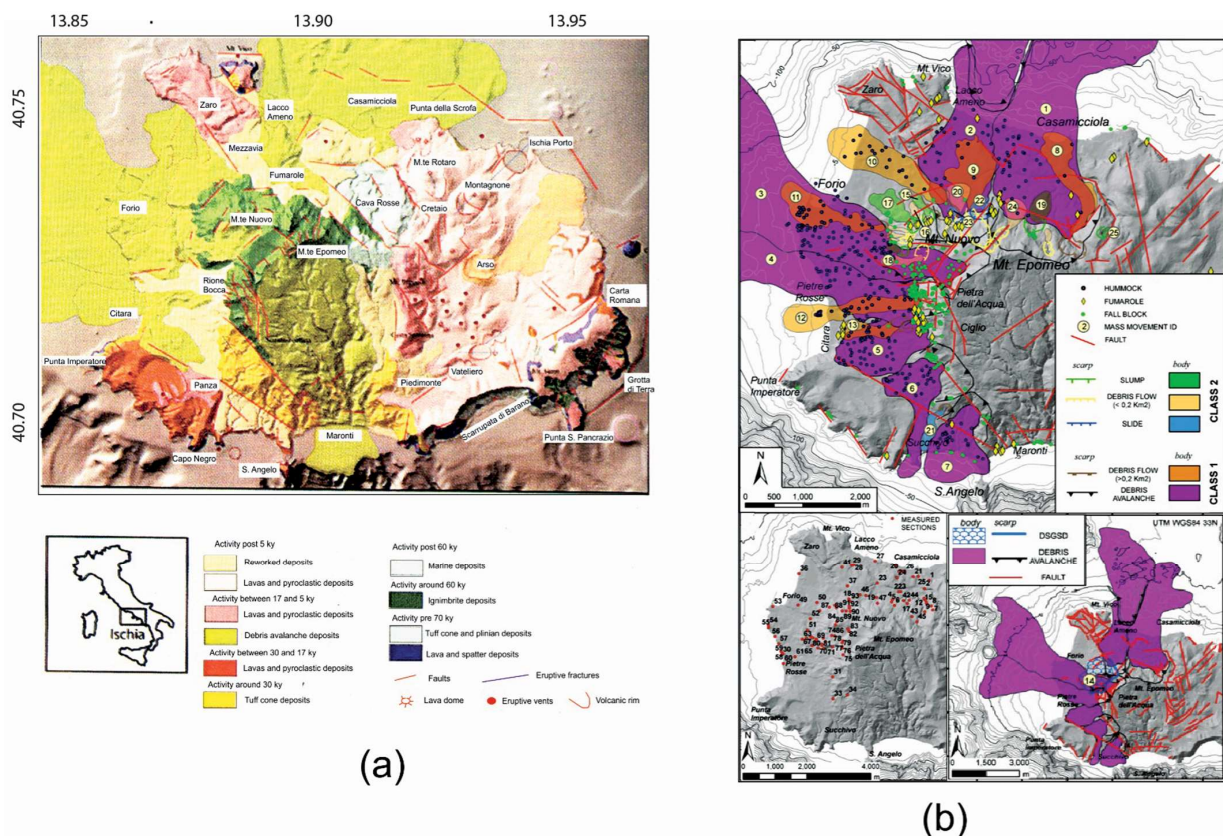


Figure 3. (a) Geologic sketch map of Ischia (modified after Sbrana et al.) [37]. (b) Onshore and offshore extension of the Epomeo Mt. gravitational landforms and offshore extension of the debris avalanche deposits (modified after Della Seta et al.) [38].

3. Materials and Methods

A literature review has been carried out for the identification of the marine hazards of Naples Bay, regarding the earthquakes, submarine landslides, tephra deposits, pyroclastic density currents (PDC), and tsunamis. The geophysical dataset consists of multibeam and seismic data of Naples Bay and the Salerno Valley. Curiosity-driven research has been carried out for the Salerno Valley and the southern slope of the Sorrento Peninsula (Sister II oceanographic cruise, CNR ISMAR, Naples, Italy).

Detailed DEMs and bathymetric profiles have been constructed by using the Global Mapper software, TRIAL version (<https://globalmapper.it/download.php> accessed on 1 May 2024). Multichannel seismic profiles (GRNA35; oceanographic cruise GMS00_05; CNR ISMAR, Naples, Italy) and Sparker seismic profiles recorded for the marine geological survey of the Ischia Island at the 1:10.000 scale have been interpreted. Multichannel seismic acquisition was carried out at a constant distance interval of 6.25 m, with a receiver interval of 6.25 m, a minimum offset of 130 m, and a fold of 1200%. The data recorded by the hydrophones have been acquired using the Stratavisor NX (Geometrics Inc., San Jose, CA, USA), recording 24 channels. Sparker seismic acquisition was performed using a multi-tip sparker system (SAM96 model), whose technical characteristics include short pulse lengths and increasing peak pressure. This sparker system generated 200 J in the 200–2000 frequency range. Seismic profiles have been interpreted by using the CorelDraw graphic suite, version 17.0 (<https://www.coreldraw.com/it/> accessed on 1 May 2024).

4. Results

4.1. Literature Review

4.1.1. Earthquakes

Vesuvius, Campi Flegrei, Ischia, and Procida are hazardous volcanoes, where seismicity occurred in recent times. In recent years, the earthquakes have been mainly controlled by the Campi Flegrei bradyseism. The eruption of the caldera has been happening for at least 10 million years. The Campi Flegrei caldera reactivation is believed to be associated with volcanism, ground deformations, and seismicity. In the uplifted section of the caldera, the volcanic edifices prevail, achieving both long-term deformation, that is to say, resurgence, and short-term deformation, that is to say bradyseism. Two main bradyseismic crises are known between 1969–1972 and 1982–1984.

Table 1 shows that significant earthquakes occurred in Campi Flegrei and Naples Bay in recent years (<https://terremoti.ingv.it/events> accessed on 1 May 2024). The earthquakes are listed by decreasing magnitude and represent a main geohazard in the Naples area. During the last year (2023), 572 earthquakes occurred at Campi Flegrei and Vesuvius based on the INGV catalog. The most significant ones (magnitude between 3 and 4) have been reported in Table 1. The earthquake of Casamicciola (Ischia) on 21 August 2017 has also been reported, due to the intense destructive effects.

Campi Flegrei earthquakes are genetically related to bradyseism. A 4.3-magnitude earthquake hit Campi Flegrei on 27 September 2023 (Table 1). It was the region's longest-lasting quake in 40 years, and it was a component of a seismic sequence that has been reverberating Campi Flegrei for a couple of weeks. To better understand these trends, Kilburn et al. [39] constructed a model to keep track of the evolution from an elastic state to an inelastic one, in which rocks begin to fracture more and more and breaking originates beneath the faults. In this scenario, the frequency of local earthquakes is directly related to the rate of ground deformation. In the first instances, the ground deformation brings about a few earthquakes, but as the stress increases in the crust, the same quantity of ground deformation, with time, quickens the frequency of earthquakes [39]. To the extent that the unrest has affected the geometry of Campi Flegrei's crust, the reported findings introduced data for forecasting the volcano's likelihood to erupt or subside prior to eruption [39].

The destructive faults located on Ischia Island controlled the Casamicciola earthquake that occurred in 2017. De Novellis et al. [40] provided an explanation of the earthquake based on an integrated geophysical study aimed at reconstructing the focal mechanisms of

the Casamicciola earthquake [40]. The obtained results revealed an E–W striking, south-dipping normal fault, which is compatible with the rheological stratification of the crust at Ischia.

Table 1. Earthquakes in the Bay of Naples (<https://terremoti.ingv.it/events> accessed on 1 May 2024).

| Time | Magnitude (Mw) | Location | Depth | Latitude | Longitude |
|-------------------|----------------|-----------------------|-------|----------|-----------|
| 27 September 2023 | 4.2 | Campi Flegrei | 3 km | 40°82′ | 14°16′ |
| 2 October 2023 | 4.0 | Campi Flegrei | 3 km | 40°83′ | 14°15′ |
| 21 August 2017 | 3.9 | Casamicciola (Ischia) | 2 km | 40°74′ | 13°90′ |
| 7 September 2023 | 3.8 | Campi Flegrei | 3 km | 40°83′ | 14°15′ |
| 16 October 2023 | 3.6 | Campi Flegrei | 2 km | 40°8′ | 14°14′ |
| 11 June 2023 | 3.6 | Campi Flegrei | 3 km | 40°83′ | 14°11′ |
| 18 August 2023 | 3.6 | Campi Flegrei | 2 km | 40°83′ | 14°14′ |
| 8 May 2023 | 3.4 | Campi Flegrei | 3 km | 40°83′ | 14°14′ |
| 22 September 2023 | 3.0 | Campi Flegrei | 1 km | 40°83′ | 14°14′ |
| 23 November 2023 | 3.1 | Campi Flegrei | 3 km | 40°83′ | 14°14′ |
| 17 February 2024 | 3.0 | Campi Flegrei | 3 km | 40°84′ | 14°12′ |

4.1.2. Submarine Landslides

In Naples Bay, submarine landslides are an important marine geohazard. Significant slides have been detected both at Ischia and in central Naples Bay, in the Dohrn and Magnaghi canyons, while creeping of the sea bottom occurs offshore at the Sarno river mouth toward the Vesuvius coastline. The N and W onshore sectors of Ischia are affected by debris avalanches [38], as well as the offshore, where hummocky deposits have been identified [33–37]. Onshore, they include a debris avalanche detached from the western flank of the Epomeo Mt. and a deep-seated gravitational deformation involving the Monte Nuovo [38]. Among the debris avalanches of Ischia, the largest one is the Ischia debris avalanche (IDA) [15].

Significant submarine slides occur in the Dohrn canyon system, where slide scars do not correspond with adjacent slide deposits, which have probably been reworked and removed by sea bottom currents [18,24,41]. During the late Quaternary, submarine slides mainly involved both the canyon's heads, being double regressive (Dohrn) and triple regressive (Magnaghi). In this area, the geological evolution of submarine slides has been explained according to the three-stage model of Pratson and Coakley [42] for submarine canyon evolution [43]. This approach is centered on the modification of the slope failures in a canyon with a retreating head, receding upward on the slope along the pre-canyon channels, as dictated by the retrogressive slides modulated by strong volcanoclastic input. The first phase, corresponding to the carving of the pre-canyon channels, happened in a time interval ranging between 37 ky B.P. (eruption of the Campanian Ignimbrite) and 15 ky B.P. (eruption of the Neapolitan Yellow Tuff). The second phase, corresponding to the canyon development through slope failures, happened later than 15 ky B.P. (eruption of the Neapolitan Yellow Tuff) [43]. The third stage, corresponding to the individuation of the canyon retrogressive heads, is older than the growth of the Nisida volcanic bank (Naples offshore), physically interrupting the Dohrn western branch (4.8–3.8 ky B.P.) [43]. Figure 4 shows the high-slope map of Naples Bay, which was previously constructed [24], identifying the areas prone to slide, which are those having gradients greater than 10°.

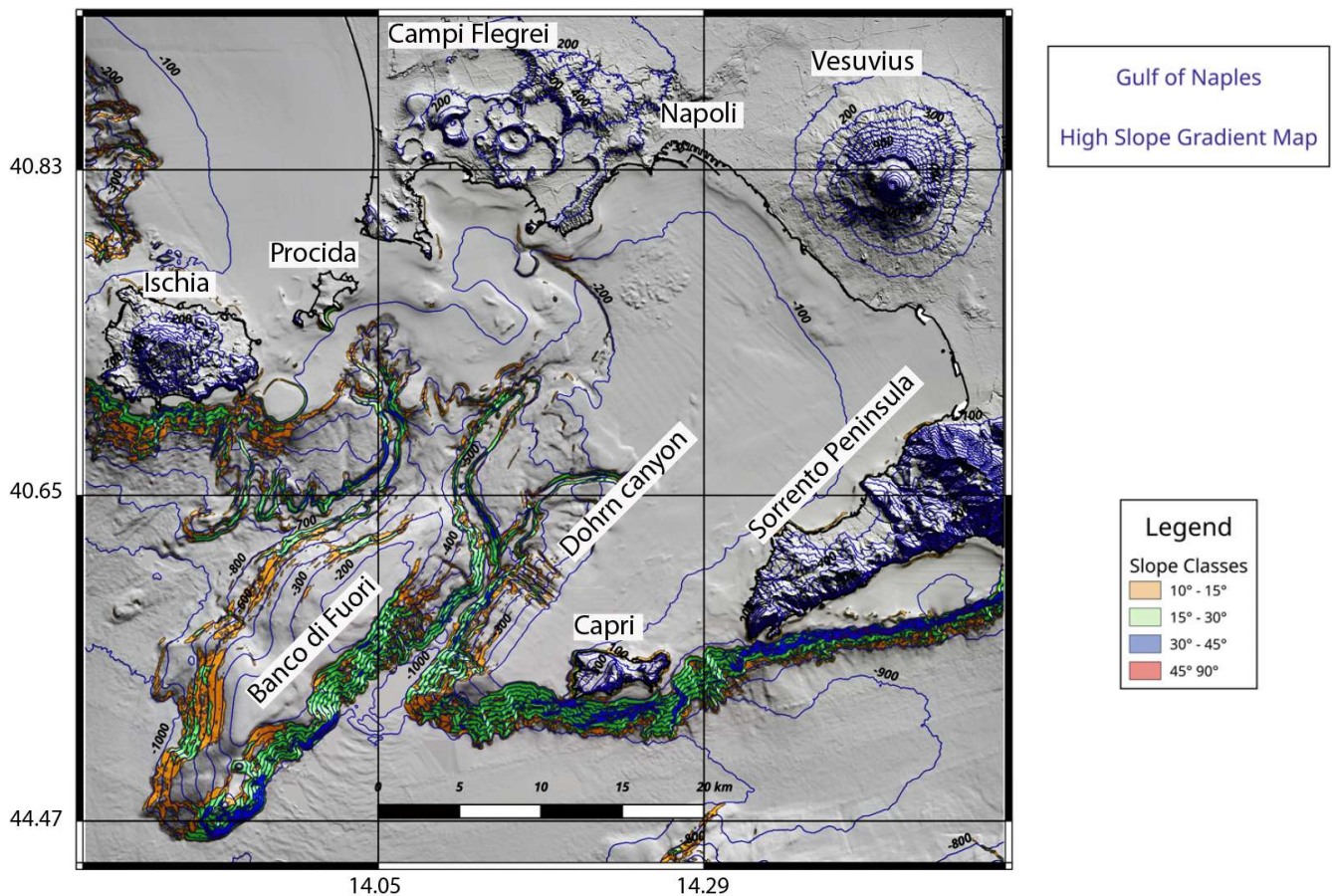


Figure 4. High-slope map of Naples Bay, showing marine areas potentially prone to slide (modified after Aiello and Sacchi [24]).

4.1.3. Marine Tephra

Marine sediment cores enclosing tephra provide reliable datasets for volcanic and marine hazards [44]. Satow et al. [44] highlighted that the marine sediment cores give detailed information on long-term hazard assessment, being archives of volcanic activity. They include ash (tephra) deposits, cryptotephra deposits, pyroclastic density current (PDC) deposits, and reworked volcanoclastic deposits, giving detailed geologic and volcanologic information on marine hazards.

Many studies have been carried out in the Bay of Naples regarding the marine tephra layers, providing information on the marine and volcanic hazards, both at Ischia [45–50] and on the Naples continental shelf [12,51–53]. The reconstructed stratigraphic model provides improved estimates of future eruption hazards, such as plume height and the total volume of eruptive material.

Brown et al. [45] established the general stratigraphic setting of the southeastern Ischia tephra. De Alteriis et al. [46] recognized two collapse events of the IDA, including the Ischia submarine debris avalanche/debris flow (DA/DF), dated between ~3 ka B.P. and 2.4 ka B.P., and a former, pre-Holocene, DA/DF older than 23 cal ka B.P. De Vita et al. [47] examined the impact of the Ischia Porto tephra, consisting of a poorly dispersed pyroclastic deposit, on the Greek settlements of Ischia, based on recent excavations on S. Pietro Hill, eastward of Ischia harbor.

Tomlinson et al. [48] analyzed the distal tephra layers of Ischia, spanning a time interval between 104 and 39 ky B.P., which yielded proximal–distal trends for a broad spectrum of eruptions. Primerano et al. [50] reconstructed the Cretaio tephra fallout dispersal, which is larger than previously known and extends from Naples Bay to the middle of the Tyrrhenian

Sea at the latitudes of the Cilento Promontory, as shown by the map of the ground deposit isomass lines (Figure 5A).

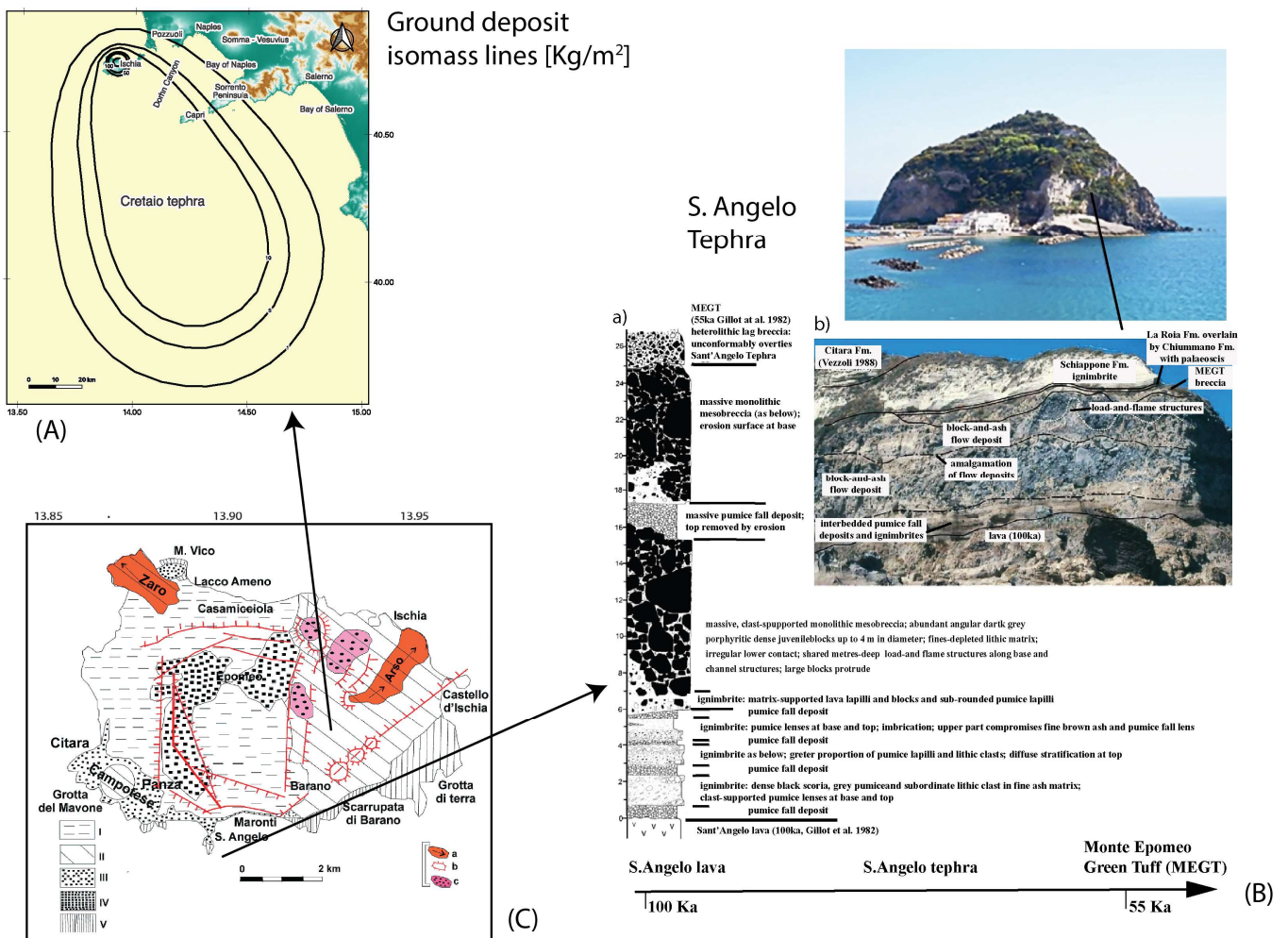


Figure 5. (A) Ground deposit isomass lines (kg/m²) on domain covered by Cretaio tephra (Tyrrhenian Sea; modified after Primerano et al. [50]). (B) S. Angelo tephra of Ischia (modified after Brown et al. [45]) (a) Sketch stratigraphic column of the tephra. (b) Significant outcrop of the S. Angelo tephra. (C) Location of the Cretaio and S. Angelo tephra superimposed on the geological map of Ischia. Key. I scree and mud flows; II volcanic units younger than 10,000 years; III older volcanic rocks (between 20,000 and 33,000 years ago); IV Green Tuff of Mount Epomeo; V first volcanic complex, now dismantled (including the first and the second phase of Ischia activity).

In the Bay of Naples, marine tephra deposits have constrained the eruption magnitude and frequency in the area, as well as the distribution of pyroclastic deposits associated with the most recent activity of Vesuvius [51–53], thereby improving the knowledge on marine hazards.

Core data have shown that the 79 AD Vesuvius tephra, interstratified in the Quaternary marine succession (Figure 6) [51–53], has a thickness ranging between 90 and 40 cm next to the Sarno Plain (C81, C82, C4) and 10 cm next to the shelf margin of Naples Bay (C69). Figure 6 shows that the tephra is located below younger marine deposits.

In the proximal areas, the tephra deposits consist of coarse-to-medium-grained sands and gravels. In the distal areas, it consists of sandy silts with fine-grained lithic and bioclastic components [43,51–53] (Figure 6).

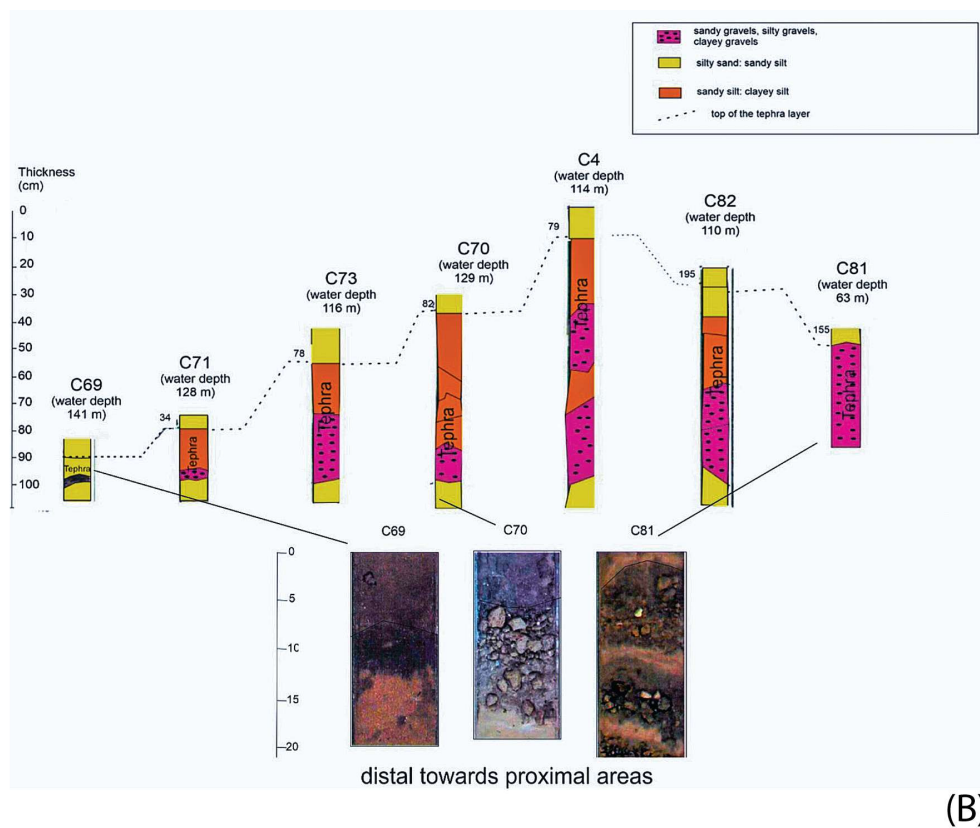
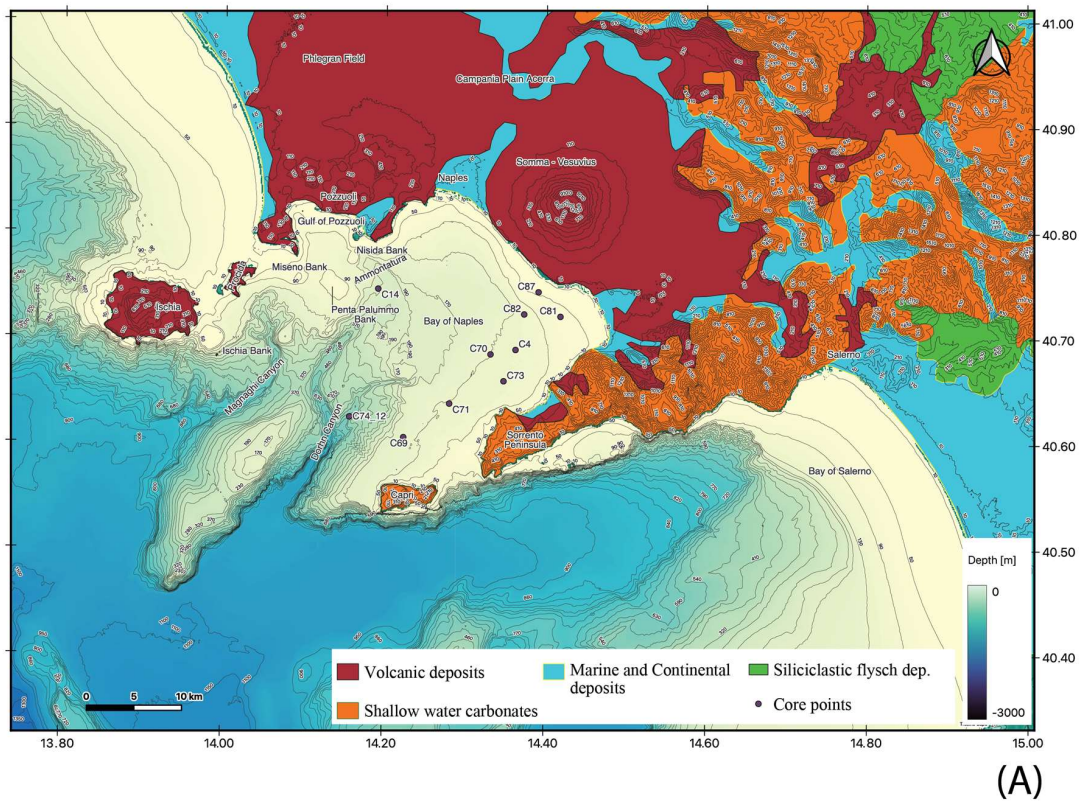


Figure 6. (A) Location map of the cores showing marine tephra in Naples Bay (modified after Aiello and Caccavale [43]). (B) Sketch stratigraphic section of the C69, C71, C73, C70, C4, C82, and C81 cores [51–53], in which the top of the tephra layer has been reported, and detailed core photographs showing the passage from distal (fine-grained) to proximal (coarse-grained) areas.

4.1.4. Pyroclastic Density Currents

Pyroclastic density currents (PDCs) are the most damaging phenomena that arise during explosive eruptions. These flows of ash and debris are spreading at travel speeds of hundreds of meters per second, reaching many tens to hundreds of kilometers from the starting point. These currents tend to be erratic, and as they move forward, they transform in type between dense, clastic flows and dilute ash- and gas-rich surges, capable of dispersing from the main body of the flow and overthrowing topography.

PDC deposits are widespread in the Bay of Naples during the late Quaternary. At Ischia, forty-seven eruptions have occurred during the last 10 ky, generating PDC deposits, mainly composed of ash surges [54]. The PDC deposits of Ischia were mainly deposited in the eastern portion of the island, and the corresponding hazards have been discussed by Alberico et al. [55], who constructed maps of the frequency of the PDC invasion.

All the Plinian eruptions of Vesuvius have emplaced important pyroclastic density current (PDC) deposits. The correlation of the seismic unit with the fallout deposits representing the base of the AD 79 eruption has been made by checking the dispersions of these PDCs, corresponding with the seismic unit, on isopach maps of the “Pomici di Mercato” and “Pomici di Avellino” deposits, which are available in the volcanological literature of the area [56–61].

In addition, the PDC deposits of the “Pomici di Mercato” are roughly concentrated along the northern flanks of Mt. Somma, suggesting that the caldera was established in a geographic location that is comparable to today’s Vesuvius edifice. However, the location of the outcrops of the “Pomici di Mercato”, in correspondence with the Sebeto Plain and along the Tyrrhenian coastline, fits well with the location of a seismic unit located offshore and has been identified on seismic profiles [62]. Instead, the PCD deposits of the “Pomici di Avellino” have a maximum thickness in the western area of the volcano. An important new seismic unit recognized offshore of the Somma-Vesuvius [62] has been correlated with the fallout deposits representing the base of the AD 79 eruption of the Vesuvius volcanic sequence [56–61].

Pyroclastic flows can flow into the seawater, propagate, and reach elevated temperature levels for vast regions underwater because of the discovery of ignimbrites in marine sedimentary formations [63–68]. Sparks et al. [64] reported that the underwater habitats are more ideally suited to the welding process than many terrestrial locations. At relatively small water depths, when water and hot ash come into contact at the boundary of a flow, they can spark an explosion and cause some strong flows to be destroyed. The prerequisites for the escape of a pyroclastic flow into deep water usually involve steep slopes and a huge rate of flow. Trofimovs et al. [65] observed the behavior of pyroclastic flows entering the sea, when 90% of the total material was deposited into the submarine settings. When the main flow enters into the sea, phreatic explosions occur, and a surge cloud originates. The coarse-grained components of the flow are deposited in proximal environments, while the fine-grained components are elutriated in the upper part of the flow, forming a turbidity current. Di Capua and Groppelli [66] showed that the PDCs that interact with the water usually experience physical alteration, producing flow dispersal and reorganization in cold, water-supported turbidites. In any case, the reliability of primary volcanic structures has been fully attested in shallow waters. A geological survey and laboratory analysis concluded that the granular flow-dominated scenarios describe the most suitable flow mechanism conditions of the pyroclastic flows in the Val d’Aveto Formation [66]. Clare et al. [67] showed that the immediate release of huge quantities of erupted solids onto steep undersea slopes created fast seafloor flows. These density currents were more rapid than those brought on by earthquakes, floods, or storms. Maeno and Imamura [68] highlighted that for the pyroclastic flow hypothesis, two sorts of two-layer shallow water simulations, dense- and light-type models, were employed owing to divergent launch scenarios in the Krakatau eruption of Indonesia. It is worth noting that this kind of two-dimensional model has still not been applied to the PDCs of the Bay of Naples, and further work is required for the volcanologists.

Milia et al. [63] explained the effects of the pyroclastic fluxes in Naples Bay. In particular, these authors constructed a map showing the main pyroclastic fluxes entering the sea in Naples Bay (Figure 7). These fluxes have been represented by the isopachs of the AD 79 pumice fall deposits and pyroclastic flow deposits (Figure 7). An undersea volcanoclastic fan that has its roots in the AD 79 eruption of Vesuvius stands for the resiliency of the PDCs that fossilized the Roman village of Herculaneum (Pompeii). This fan represents a well-documented stratigraphic record of PDCs that erupted on the continental platform in a shallow water setting, as controlled by syn-depositional reworking through wave action.

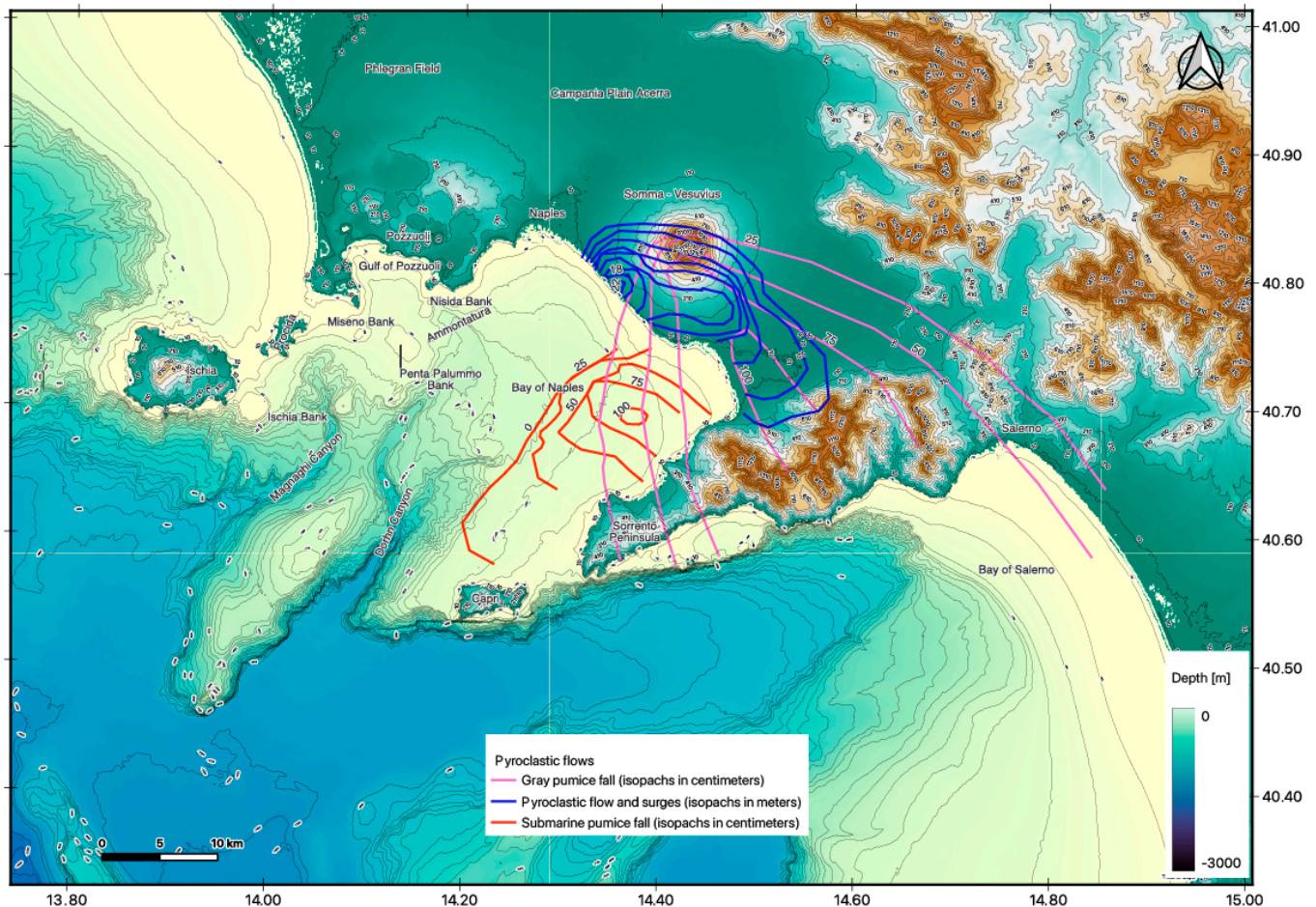


Figure 7. Pyroclastic flows related to the AD 79 eruption in Naples Bay (modified after Milia et al. [63]).

4.1.5. Tsunamis

In Naples Bay, tsunamis constitute a severe geohazard due to their close relationships with the volcanic eruptions, earthquakes, and submarine landslides [19–22,69–73]. Historical tsunamis have also been documented, including the 1343 tsunami affecting Tyrrhenian Sea, including the Bay of Naples [71,73]. This tsunami destroyed many harbors, including Amalfi, and has been documented by historical sources [73]. This event could be genetically related to the flank collapse of the Stromboli volcano [71]. Analyzing the proportions of tsunamis caused for different reasons in Naples Bay is still a complicated matter and requires further study. For the models known in the previous literature, only numerical simulations have been carried out, and the explanation of different proportions of tsunamis is not certain. Tinti et al. [19] studied the triggering of a tsunami and its propagation in Naples Bay, which was controlled by Vesuvius pyroclastic flows. A finite-element model has been used for the simulation, showing that the oscillations are larger in the gulf and more negligible proceeding basin-ward (Figure 8a) [19]. Di Fiore et al. [41] evaluated the

tsunami and wave run-up in the Dohrn canyon, showing a detachment area of about 415 m across at water depths ranging between -250 m and -370 m (Figure 8b) [41]. The obtained results have shown that the amplitude wave run-up, expressed in terms of depth of seafloor percentage, varies from 0 to 2.5%, and the wave height amplitude corresponds to 5–6 m (Figure 8b) [41]. Tinti et al. [20] simulated the tsunami triggered by the IDA [13], showing that on Ischia, the wave amplitudes exceed 40 m, while Capri is reached by the wave after about 8 min by relevant waves (Figure 8c) [20]. Alberico et al. [69] analyzed the tsunami vulnerability of the city of Naples, which is composed of the water vulnerability and structural vulnerability. A high structural vulnerability characterizes the Chiaia area close to the shoreline and the eastern sector of the Sebeto-Volla plain, whereas in the western sector, this area is controlled by the presence of a 70 m structural height, preventing the onshore propagation of tsunami waves.

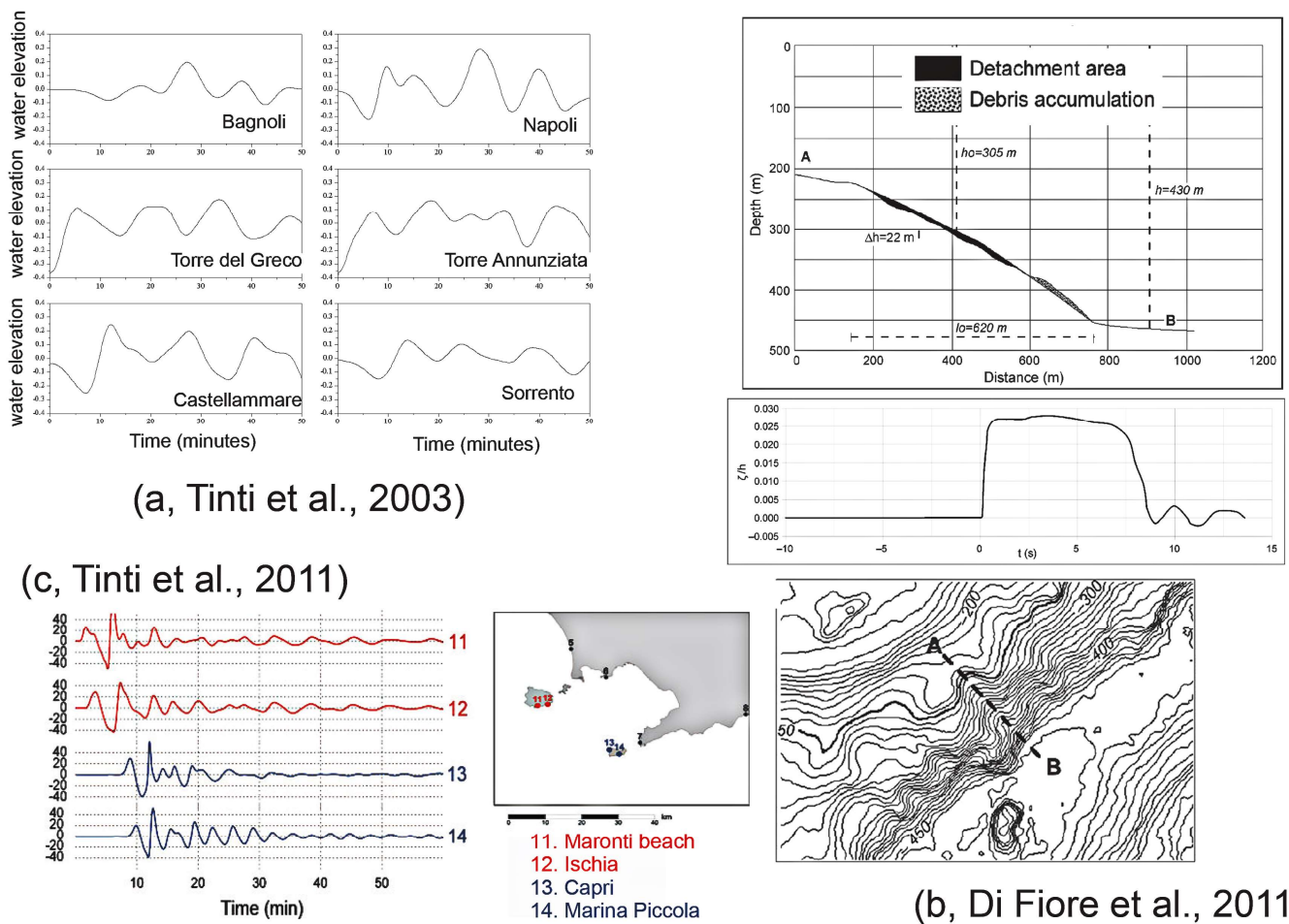


Figure 8. Mareograms related to tsunami in Naples Bay ((a), modified after Tinti et al. [19]), ((b), modified after Di Fiore et al. [41]), and Ischia ((c), modified after Tinti et al. [20]). In sub-figure (b), h_0 is the characteristic water depth, h is the water depth, and ζ is the free surface displacement. In sub-figure. AB is the bathymetric profile. (c), the modeled tsunami refers to Ischia as controlled by the Ischia debris avalanche (IDA) [15].

4.2. Morpho-Bathymetric and Seismo-Stratigraphic Analysis

4.2.1. Ammontatura Slope Basin

The detailed digital terrain model (DTM) and bathymetric profiles are herein revised (Figure 9). The center of the Bay of Naples is outlined by the Ammontatura channel, which is the seabed physiographic expression of the Ammontatura slope basin. The channel is 2.5 km wide and 20–40 m deep. The DTM and bathymetric profiles have displayed

that this channel shows a curved form, a smooth thalweg, and unbalanced scarps. This channel splits the “Banco della Montagna” feature from the volcanic brinks of Campi Flegrei. Bathymetric profiles demonstrate that the western slope of the Ammontatura channel is broadly more precipitous than the eastern one. In its northernmost part, the pivot of the channel flexes toward the northwest and shortly aborts N of the Nisida Bank (Figure 9).

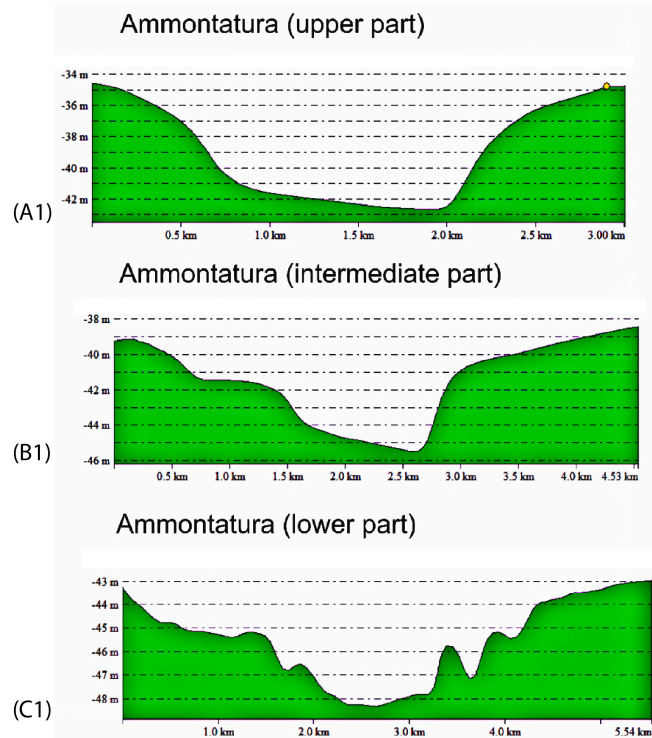
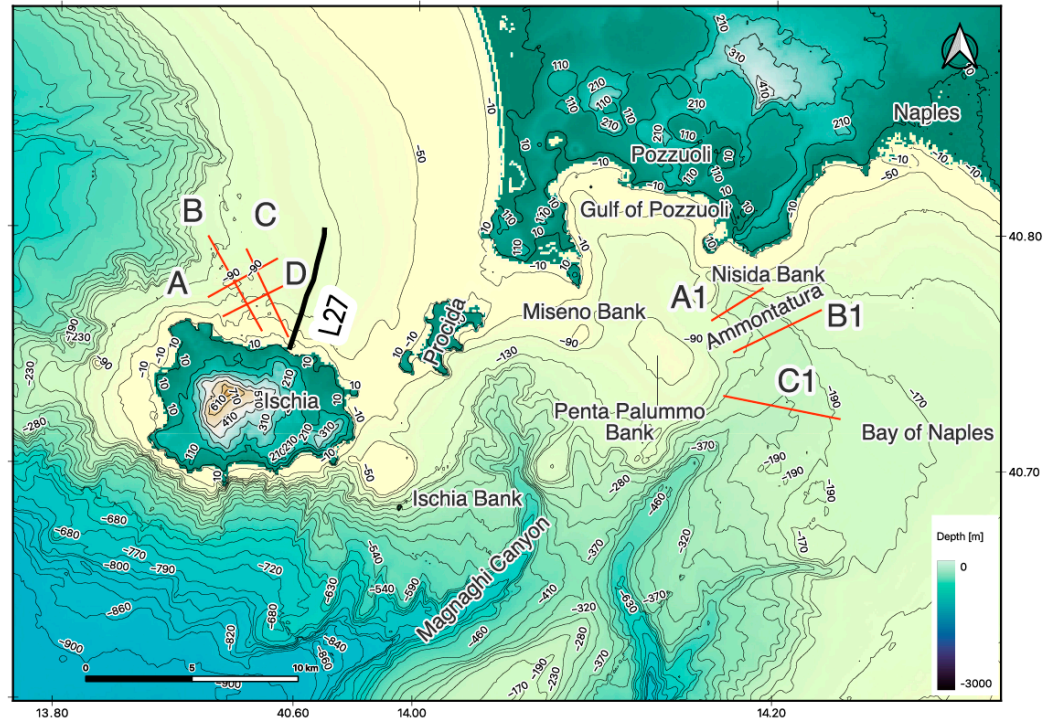


Figure 9. Detailed DEM and bathymetric profiles of the Ammontatura slope basin (modified after Aiello et al. [16]) A–D/A1–C1 indicate the bathymetric profiles.

The seismic profile GRNA35 has shown the stratigraphic architecture of the Naples Bay continental shelf (Ammontatura Channel; Figure 10); un-interpreted and interpreted seismic sections have been provided (Figures 10 and 11). The geological interpretation of the GRNA35 seismic profile showed that the Ammontatura slope basin contains two important volcanic seismic units, i.e., the Campanian Ignimbrite (CI) and the Neapolitan Yellow Tuff (NYT; Figure 11). In the two coastal and marine seismic units, which are late Pleistocene and Holocene in age, volcanoclastic sedimentation is significant. The CI deposited during isotopic stage 3, while the NYT deposited during the upper part of isotopic stage 2, corresponding to the transgressive system tract (TST) in Naples Bay. The late Pleistocene coastal and marine deposits correspond with the TST, while the overlying Holocene coastal and marine deposits represent the highstand system tract (HST). The NYT seismic unit is deformed in the Banco della Montagna structure, a volcanoclastic field located in the Naples Bay continental shelf (Figures 10 and 11).

4.2.2. Northern Ischia Debris Avalanche Deposits

The northern Ischia debris avalanche deposits are discovered in a submarine region from 20 to 180 m and include large blocks, cropping out at the seabed or fossilized by Holocene deposits. A detailed shaded relief map of the northern Ischia debris avalanche deposits is reported in Figure 12. The physiographic expression at the seabed of the northern Ischia debris avalanche deposit is represented by blocks having variable dimensions immersed in a pelitic matrix (Figure 12). The western and eastern boundaries of the deposits have been identified. While the western boundary of the deposits is located next to the M.te Vico structure, the eastern one extends up the Punta La Scrofa promontory.

The structure of the northern Ischia debris avalanche deposit has been studied through four bathymetric profiles (Figure 13). The first profile crossed the distal part of the deposit with an NE–SW trend. The main accumulation of the deposit rises to the seabed to 60 m of water depth. Its sides are characterized by two channelized areas located at water depths of 110 m. The first one rises to water depths of 100 m; the second one, about 4 km wide, reaches water depths of 90 m (Figure 13).

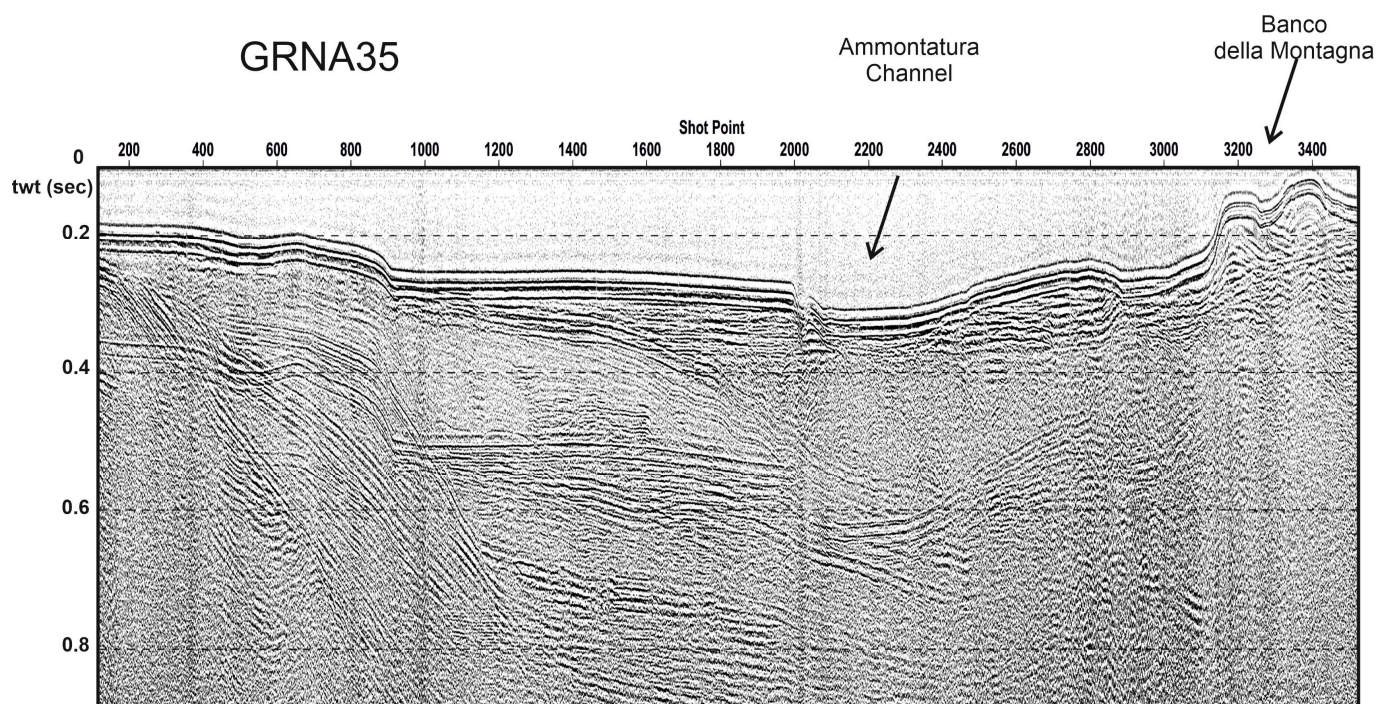


Figure 10. Seismic profile GRNA35, crossing the Ammontatura channel.

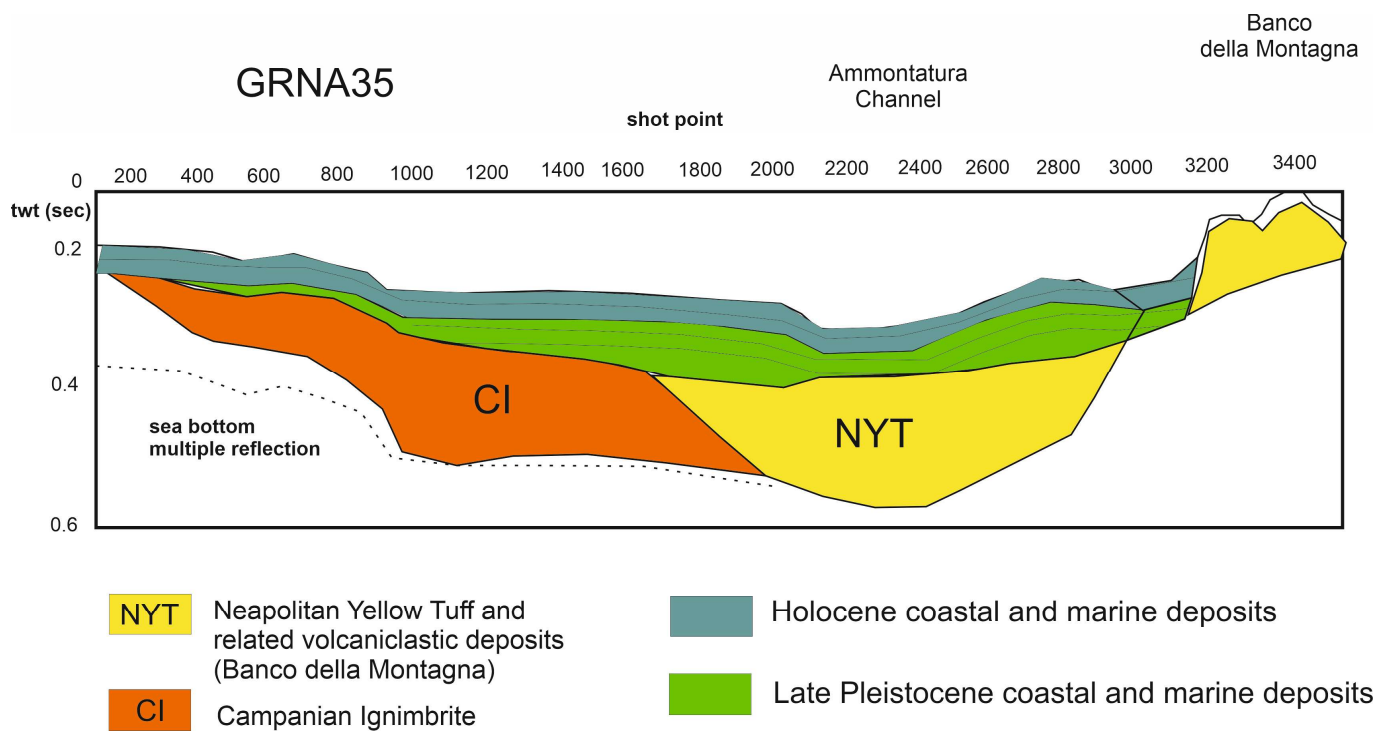


Figure 11. Geological interpretation of the seismic profile GRNA35, crossing the Ammontatura channel.

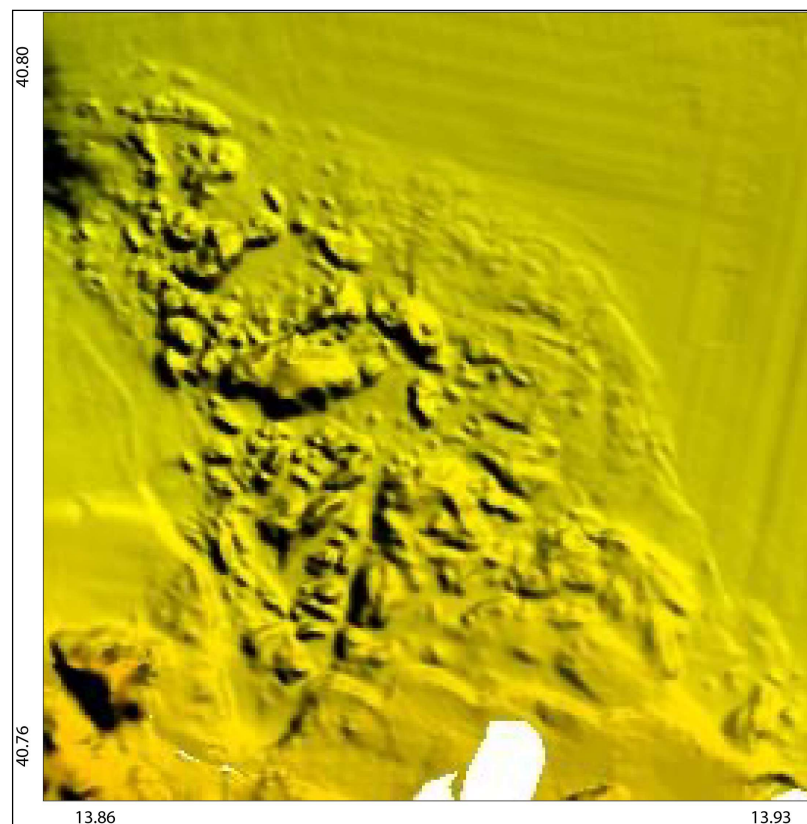


Figure 12. Detailed DEM of the northern Ischia debris avalanche.

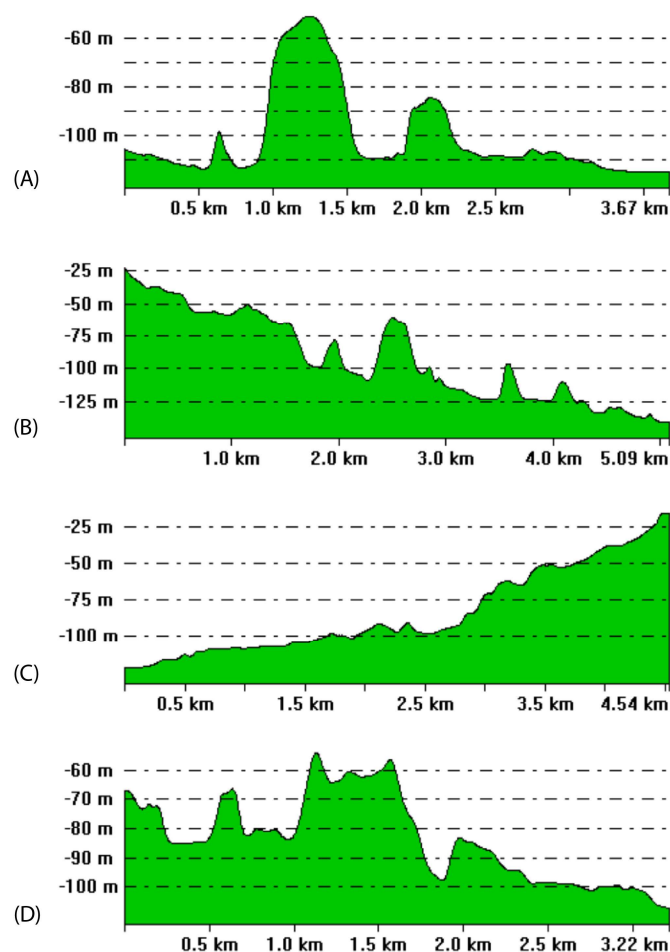


Figure 13. Bathymetric profiles in the northern Ischia debris avalanche deposits (A–D) represent the bathymetric profiles.

The second bathymetric profile crosses the northern Ischia debris avalanche deposit longitudinally with an NNW–SSE trend at water depths ranging between 25 m and 130 m. The profile shows the irregularly articulated structure of the deposit, 1.8 km wide, with a channel bounded by levees at water depths of 55 m. Proceeding seaward, after a break in slope at 70 m, the deposit is carved by two deep channelized areas, located at water depths of 100 m. Further out, another accumulation exists, 500 m wide, whose top reaches 70 m of water depth (Figure 13).

The third profile runs in the deposit longitudinally, with an SSW–NNE trend. For a distance of 3 km, the topography of the deposit rises to 70 m of water depth. In this area, several channels occur, having variable entity and amplitude, carving the deposit. Starting from 70 m, the deposit develops up to 25 m, showing two main channels along its topographic profile (Figure 13).

The fourth section has shown that the main deposit occurs at the center of the section at water depths of 60 m and is bounded by two channels, respectively located at water depths of 80 m (on the left of the deposit) and 95 m (on the right of the deposit). Two other culminations of the deposit, respectively located at 70 m and 85 m of water depth, occur (Figure 13).

The northern Ischia debris avalanche deposit is crossed by seismic profile L27. The deposit is organized into two distinct superimposed bodies (H1 and H2; Figure 14). The basin filling is composed of three seismo-stratigraphic units (C, D, E), partly in facies heterogeneity with the upper part of buried volcanic structures, acoustically transparent, and characterized by a dome-shaped external geometry (Figure 14).

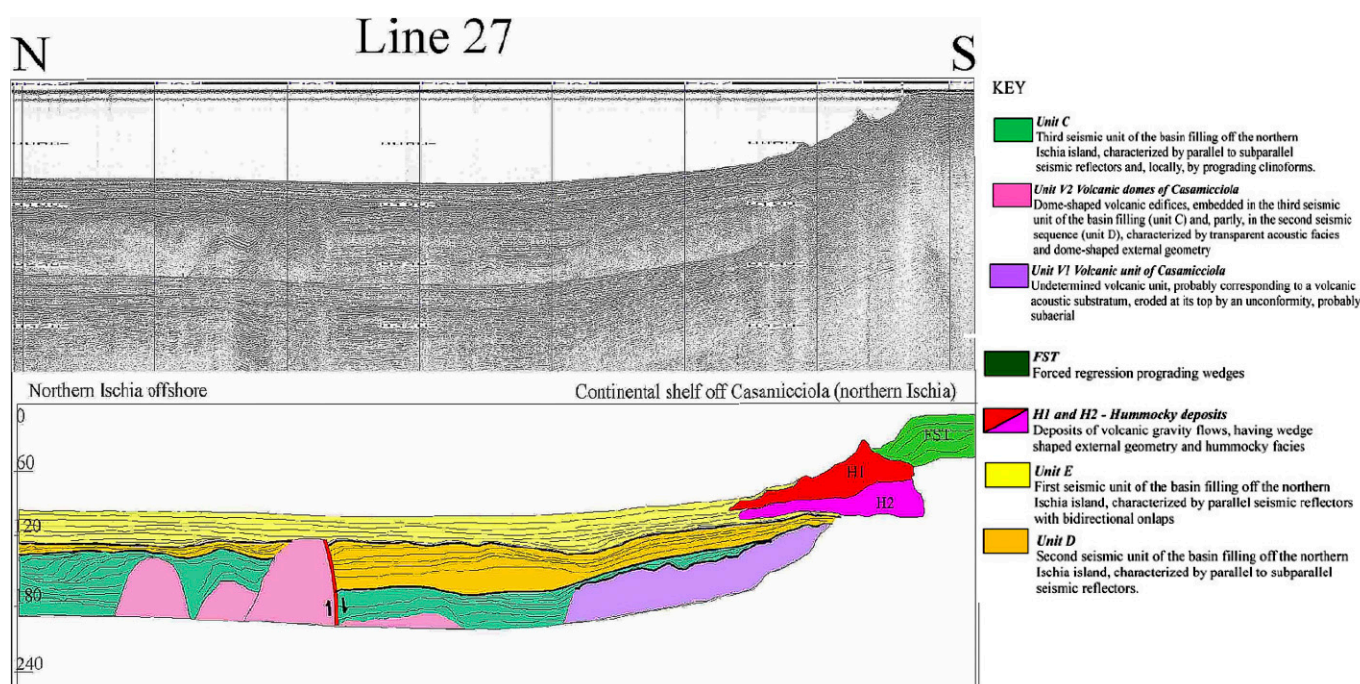


Figure 14. Seismic profile in the northern sector of Ischia (Casamicciola) and corresponding geological interpretation.

5. Discussion and Conclusions

We made use of high-resolution bathymetry maps to assess the morphological pattern of the sea and establish the related marine hazard. Naples Bay is continually exposed to high-intensity human impacts that contribute to coastal zone stress and a broad range of natural hazards, such as seismicity, volcanic activity, gravity slides, pyroclastic density currents, and tsunamis. It is an area of about 900 km² that is part of the Campania region, which is one of the geographical regions of the world that is most vulnerable to a significant volcanic hazard because it is a densely human-populated area. The volcanic hazard is strictly associated with the reactivation of the magmatic systems of the Phlegrean Fields, Somma-Vesuvius, and Ischia Island. Ground deformation is particularly severe at the Phlegrean Fields and Ischia Island, where divergent tectonic uplift is modulated by the growth of volcano-tectonic faults and hydrothermal systems. Seismic and bradyseismic crises dominate the Phlegrean Fields, where an uplift of 1.8 m from 1982 to 1984 caused the evacuation of about 30,000 people from the town of Pozzuoli, and an actual bradyseismic crisis is still in course. Ischia has undergone, in historical times, natural seismic activity and lateral collapses. The most recent one is the Casamicciola earthquake of 2017.

Detailed marine geohazard maps of the Bay of Naples have been constructed, taking into account geomorphological data and maps that were previously obtained [24] (Figure 15). The obtained results have shown the suitability of the morpho-bathymetric and seismo-stratigraphic studies when applied in studying both volcanic and sedimentary depositional environments in the Bay of Naples, as well as that the marine hazard is higher in three districts, including the Ischia slope, the Naples canyons, and the Sorrento slope (Figure 15).

In the Ammontatura slope basin, the morpho-bathymetric and seismic data have shown a close relationship with the Dohrn canyon and the important seismic units of Naples Bay (CI and NYT; Figure 11). A significant contribution of volcanoclastic sedimentation in the Holocene marine sedimentation is suggested by sedimentological and tephrostratigraphic data on the Bay of Naples. The Ammontatura channel is a fossil branch of the Dohrn canyon, genetically related to the western branch, draining the volcanoclastic input of Campi Flegrei and Procida eruptions. The occurrence of tephra having a Phle-

graeen provenance in the core data [51–53] supports this working hypothesis, which is still in the course of study. The growth of the volcanic edifice of the Nisida Bank post-dates the activity of the Ammontatura channel, abruptly ending on the volcanic edifice. The Ammontatura slope basin and related channel were active during a time interval spanning between the NYT eruption (15 ky B.P.) and the growth of the Nisida Island and Nisida Bank (4.8–3.7 ky B.P.).

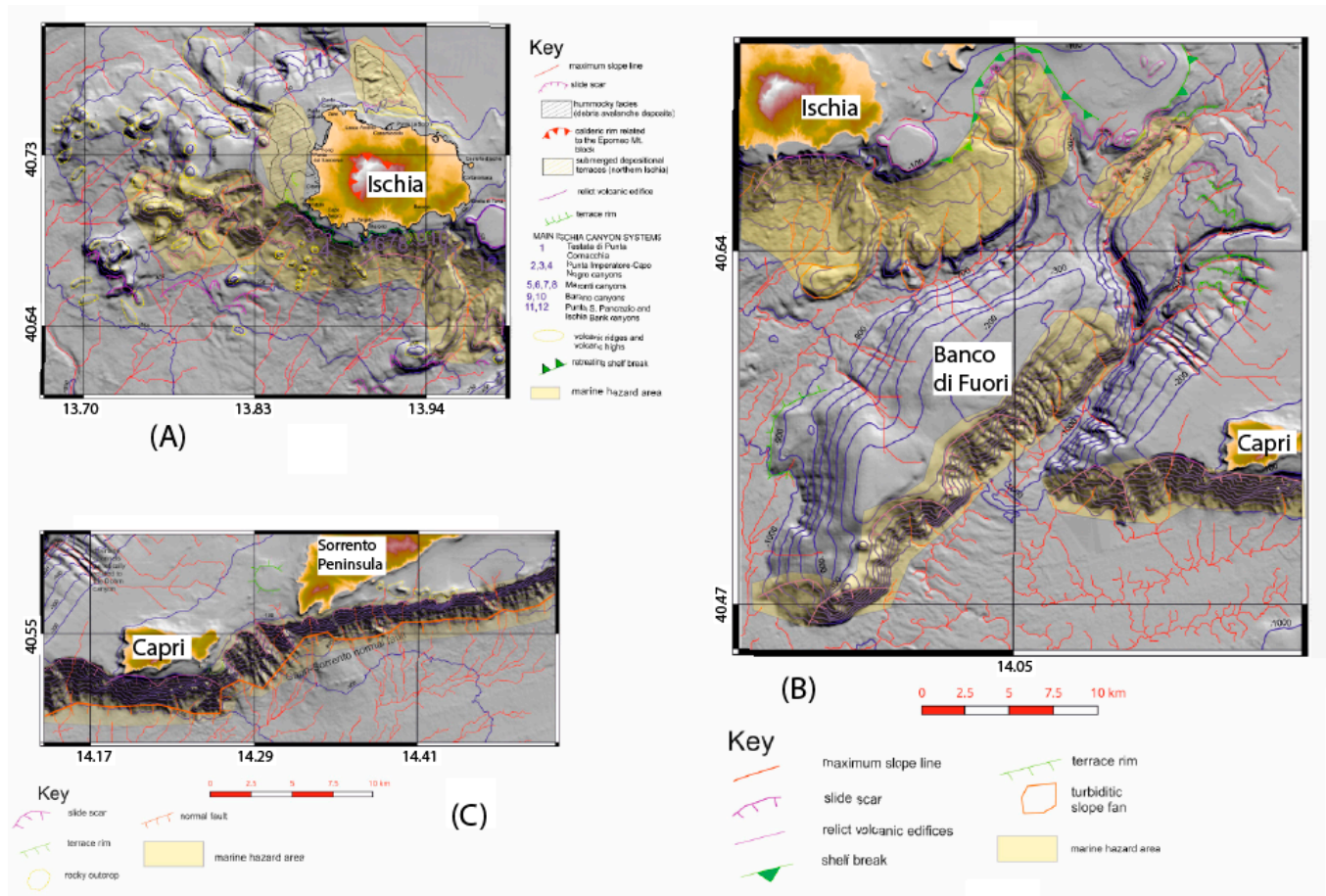


Figure 15. Detailed geomorphological maps of Naples Bay showing marine hazards (in yellow). (A) Ischia; (B) Naples canyons, (C) southern slope of the Sorrento Peninsula (modified after Aiello and Sacchi [24]).

The southern slope of the Sorrento Peninsula is a tectonically controlled slope governed by the Capri–Sorrento normal fault. Our data have shown a dense network of drainage channels. The platform margin is incised by a dense network of drainage lines (Figure 15), which in some way, could reflect the drainage network occurring onshore, also if a physical continuity does not exist, because the channels start from the shelf break and do not continue in the narrow shelf off southern Sorrento Peninsula. These channels are the present-day and recent preferential transport routes of sediments entering the Salerno Valley.

Offshore of the Sorrento Peninsula, the debris flow and stream deposits, which are late Holocene in age, are composed of middle-to-fine-grained pelitic sands, with abundant plant remnants and anthropic debris. Moreover, they consist of pelitic middle-to-fine-grained sands, elongated according to maximum slope lines at the seabed or as channel fillings. The depositional areas are the portions of seabed surrounding the stream mouths along the southern slope of Sorrento Peninsula (Amalfi), oriented perpendicularly to the depositional elements of the continental shelf. This lithofacies is similar to the stream deposits located at the mouth of the Bonea stream (Salerno) and has been deposited by hyper-concentrated

fluxes following exceptional alluvial events, such as those of Vietri sul Mare and Maiori in 1954.

The northern Ischia debris avalanche deposits can be put in the frame of the eruptive activity of Ischia. A chronostratigraphic diagram of Ischia has been constructed to improve the discussion on the obtained data, also showing the stratigraphic relationships with the corresponding units of Procida (Figure 16).

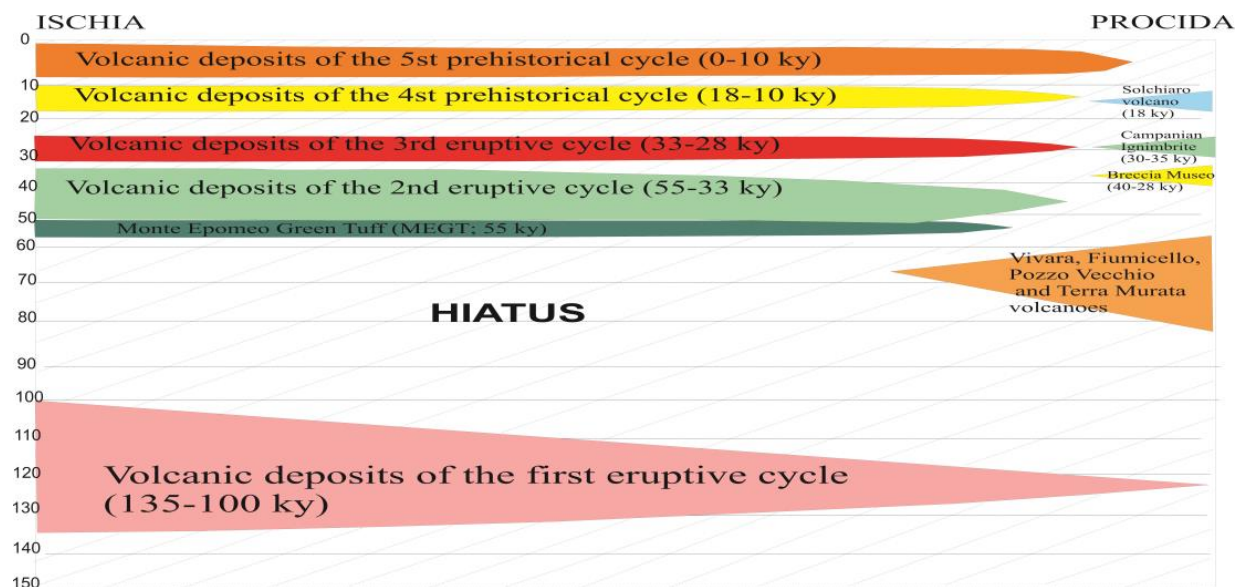


Figure 16. Qualitative chronostratigraphic diagram of Ischia. The decrease in triangles is due to the decrease in the thickness of the volcanic deposits.

The northern Ischia debris avalanche can be put in the stratigraphic framework of the fifth prehistorical cycle (0–10 ky B.P.; Figure 16). Chiocci and de Alteriis [15] explained that the Southern Ischia debris avalanche was due to a large-scale prehistorical collapse. Della Seta et al. [38] suggested that the subaerial debris avalanches of Ischia have mostly occurred since 3 ky B.P. (Figure 3b). They are associated with other gravitational mass movements, including debris flows (lahars), rock falls, slumps, debris and rockslides, small debris flows, and deep-seated gravitational slope deformation [38]. The recognition of submarine deposits genetically related to subaerial deposits highlights that the debris avalanches impacted the sea. Based on our data, we can suggest that the Northern Ischia debris avalanche deposits were deposited during two phases (H1 and H2 in Figure 14) and are not associated with an evident slide scar on land, which is in contrast with the IDA [15], which is associated with a large scar of the southern flank of the island.

Author Contributions: Formal analysis, G.A. and M.C.; investigation, G.A.; writing—original draft preparation, G.A. and M.C.; writing—review and editing, G.A. All authors have read and agreed to the published version of the manuscript.

Funding: This research received no external funding.

Conflicts of Interest: The authors declare no conflicts of interest.

References

1. Kopp, H.; Chiocci, F.L.; Berndt, C.; Çağatay, M.N.; Ferreira, T.; Fortes, C.J.E.M.; Gràcia, E.; González Vega, A.; Kopf, A.; Sørensen, J.; et al. *Marine Geohazards: Safeguarding Society and the Blue Economy from a Hidden Threat*; Position Paper 26 of the European Marine Board; European Marine Board IVZW: Ostend, Belgium, 2021; pp. 1–100. ISBN 9789464206111. [CrossRef]
2. International Centre for Geohazard. Offshore Geohazards. 2003. Available online: <https://www.yumpu.com/en/document/view/4725434/offshore-geohazards-ngi> (accessed on 1 May 2024).
3. CIESM. *Marine Geo-Hazards in the Mediterranean*; CIESM Workshop Monographs; CIESM: Monte Carlo, Monaco, 2011; Volume 42, pp. 1–192.

4. Urgeles, R.; Camerlenghi, A. Submarine landslides of the Mediterranean Sea: Trigger mechanisms, dynamics, and frequency-magnitude distribution. *J. Geophys. Res.* **2013**, *118*, 2600–2618. [[CrossRef](#)]
5. Ceramicola, S.; Praeg, D.; Coste, M.; Forlin, E.; Cova, A.; Colizza, E.; Critelli, S. Submarine Mass-Movements along the Slopes of the Active Ionian Continental Margins and Their Consequences for Marine Geohazards (Mediterranean Sea). In *Submarine Mass Movements and Their Consequences*, 1st ed.; Krastel, S., Behrmann, J., Volker, G., Urgeles, R., Chaytor, J., Huhn, K., Strasser, N., Harbitz, C., Eds.; Advances in Natural and Technological Hazards Research; Springer: Cham, Switzerland, 2014; Volume 37, pp. 295–306. [[CrossRef](#)]
6. Camargo, J.M.R.; Silva, M.; Ferreira, A.; Araujo, T. Marine Geohazards: A Bibliometric-Based Review. *Geosciences* **2019**, *9*, 100. [[CrossRef](#)]
7. Chivata Cardenas, I.; Flage, R.; Aven, T. Marine geohazards exposed: Uncertainties involved. *Mar. Georesources Geotechnol.* **2023**, *41*, 589–619. [[CrossRef](#)]
8. Wang, Y.; Heidarzadeh, M.; Satake, K.; Mulia, I.E.; Yamada, M. A tsunami warning system based on offshore bottom pressure gauges and data assimilation for Crete Island in the Eastern Mediterranean Basin. *J. Geophys. Res. Solid Earth* **2020**, *125*, e2020JB020293. [[CrossRef](#)]
9. Heidarzadeh, M.; Gusman, A.R.; Mulya, I.R. The landslide source of the eastern Mediterranean tsunami on 6 February 2023 following the M_W 7.8 Kahramanmaraş (Türkiye) inland earthquake. *Geosci. Lett.* **2023**, *10*, 50. [[CrossRef](#)]
10. Fusi, N.; Mirabile, L.; Camerlenghi, A.; Ranieri, G. Marine geophysical survey of the Gulf of Naples (Italy): Relationship between submarine volcanic activity and sedimentation. *Mem. Soc. Geol. Ital.* **1991**, *47*, 95–114.
11. Milia, A.; Torrente, M.; Russo, M.; Zuppetta, A. Tectonics and crustal structure of the Campania continental margin: Relationships with volcanism. *Mineral. Petrol.* **2003**, *79*, 33–47. [[CrossRef](#)]
12. Insinga, D.; Molisso, F.; Lubritto, C.; Sacchi, M.; Passariello, I.; Morra, V. The proximal marine record of Somma–Vesuvius volcanic activity in the Naples and Salerno bays, Eastern Tyrrhenian Sea, during the last 3 kyrs. *J. Volcanol. Geoth. Res.* **2008**, *177*, 170–186. [[CrossRef](#)]
13. Sacchi, M.; Pepe, F.; Corradino, M.; Insinga, D.D.; Molisso, F.; Lubritto, C. The Neapolitan Yellow Tuff caldera offshore the Campi Flegrei: Stratal architecture and kinematic reconstruction during the last 15 ky. *Mar. Geol.* **2014**, *354*, 15–33. [[CrossRef](#)]
14. Sacchi, M.; De Natale, G.; Spiess, V.; Steinmann, L.; Acocella, V.; Corradino, M.; de Silva, S.; Fedele, A.; Fedele, L.; Geshi, N.; et al. A roadmap for amphibious drilling at the Campi Flegrei caldera: Insights from a MagellanPlus workshop. *Sci. Drill.* **2019**, *26*, 29–46. [[CrossRef](#)]
15. Chiocci, F.L.; De Alteriis, G. The Ischia debris avalanche: First clear submarine evidence in the Mediterranean of a volcanic island prehistorical collapse. *Terra Nova* **2006**, *18*, 202–209. [[CrossRef](#)]
16. de Alteriis, G.; Scotto di Santolo, A.; Chiocci, F.L.; Ramondini, M.; Violante, C. The Case of Ischia Underwater Debris Avalanche (Italy, Tyrrhenian Sea) and Its High Mobility. In *Engineering Geology for Society and Territory*; Lollino, G., Manconi, A., Locat, J., Huang, Y., Canals Artigas, M., Eds.; Springer: Cham, Switzerland, 2014; Volume 4. [[CrossRef](#)]
17. Milia, A. The Dohrn canyon: A response to the eustatic fall and tectonic uplift of the outer shelf along the eastern Tyrrhenian sea margin, Italy. *Geo-Mar. Lett.* **2000**, *20*, 101–108. [[CrossRef](#)]
18. Aiello, G.; Iorio, M.; Molisso, F.; Sacchi, M. Integrated Morpho-Bathymetric, Seismic-Stratigraphic, and Sedimentological Data on the Dohrn Canyon (Naples Bay, Southern Tyrrhenian Sea): Relationships with Volcanism and Tectonics. *Geosciences* **2020**, *10*, 319. [[CrossRef](#)]
19. Tinti, S.; Pagnoni, G.; Piatanesi, A. Simulation of tsunamis induced by volcanic activity in the Gulf of Naples (Italy). *Nat. Hazards Earth Syst. Sci.* **2003**, *3*, 311–320. [[CrossRef](#)]
20. Tinti, S.; Chiocci, F.L.; Zaniboni, F.; Pagnoni, G.; de Alteriis, G. Numerical simulation of the tsunami generated by a past catastrophic landslide on the volcanic island of Ischia, Italy. *Mar. Geophys. Res.* **2011**, *32*, 287–297. [[CrossRef](#)]
21. Selva, J.; Acocella, V.; Bisson, M.; Caliro, S.; Costa, A.; Della Seta, M.; De Martino, P.; de Vita, S.; Giordano, G.; Martino, S.; et al. Multiple natural hazards at volcanic islands: A review for the Ischia volcano (Italy). *J. Appl. Volcanol.* **2019**, *8*, 5. [[CrossRef](#)]
22. Grezio, A.; Cinti, F.R.; Costa, A.; Faenza, L.; Perfetti, P.; Pierdominici, S.; Grezio, A.; Cinti, F.R.; Costa, A.; Faenza, L.; et al. Multisource Bayesian probabilistic tsunami hazard analysis for the Gulf of Naples (Italy). *J. Geophys. Res.* **2020**, *125*, e2019JC015373. [[CrossRef](#)]
23. Aiello, G.; Caccavale, M. Quaternary Evolution of Ischia: A Review of Volcanology and Geology. *Appl. Sci.* **2023**, *13*, 3554. [[CrossRef](#)]
24. Aiello, G.; Sacchi, M. New morpho-bathymetric data on marine hazard in the offshore of Gulf of Naples (Southern Italy). *Nat. Hazards* **2022**, *111*, 2881–2908. [[CrossRef](#)]
25. Patacca, E.; Scandone, P. Geology of Southern Apennines. *Boll. Soc. Geol. Ital.* **2007**, 75–119.
26. Milia, A.; Torrente, M.M. Tectonics and stratigraphic architecture of a peri-Tyrrhenian half-graben (Gulf of Naples, Italy). *Tectonophysics* **1999**, *315*, 301–318. [[CrossRef](#)]
27. Conti, A.; Bigi, S.; Cuffaro, M.; Doglioni, C.; Scrocca, D.; Muccini, F.; Cocchi, L.; Ligi, M.; Bortoluzzi, G. Transfer zones in an oblique back-arc basin setting: Insights from the Latium-Campania segmented margin (Tyrrhenian Sea). *Tectonics* **2017**, *36*, 78–107. [[CrossRef](#)]
28. Malinverno, A. Evolution of the Tyrrhenian Sea-Calabrian Arc system: The past and the present. *Rend Online Soc. Geol. Ital.* **2012**, *21*, 11–15.

29. Bigi, G.; Coli, M.; Cosentino, D.; Dal Piaz, G.V.; Parotto, M.; Sartori, R.; Scandone, P. *Structural Model of Italy—Scale 1: 500.000*; CNR 1983-SELCA 1992; Consiglio Nazionale delle Ricerche: Rome, Italy, 2017.
30. Vitale, S.; Ciarcia, S. Tectono-stratigraphic setting of the Campania region (Southern Italy). *J. Maps* **2018**, *14*, 9–21. [[CrossRef](#)]
31. Iannace, A.; Merola, D.; Perrone, V.; Amato, A.; Cinque, A.; Santacroce, R.; Sbrana, A.; Sulpizio, R.; Zanchetta, G.; Budillon, F.; et al. *Note Illustrative della Carta Geologica d'Italia alla Scala 1: 50.000—Fogli 466—485 “Sorrento-Termini”*; ISPRA, Servizio Geologico d'Italia: Rome, Italy, 2015; pp. 1–201. Available online: https://www.isprambiente.gov.it/Media/carg/note_illustrative/466_48_5_Sorrento_Termini.pdf (accessed on 26 February 2024).
32. Gurioli, L.; Sulpizio, R.; Cioni, R.; Sbrana, A.; Santacroce, R.; Luperini, W.; Andronico, D. Pyroclastic flow hazard assessment at Somma–Vesuvius based on the geological record. *Bull. Volcanol.* **2010**, *72*, 1021–1038. [[CrossRef](#)]
33. Bruno, P.; de Alteriis, G.; Florio, G. The western undersea section of the Ischia volcanic complex (Italy, Tyrrhenian sea) inferred by marine geophysical data. *Geophys. Res. Lett.* **2002**, *29*, 9. [[CrossRef](#)]
34. De Vita, S.; Sansivero, F.; Orsi, G.; Marotta, E. Cyclical slope instability and volcanism related to volcano-tectonism in resurgent calderas: The Ischia island (Italy) case study. *Eng. Geol.* **2006**, *86*, 148–165. [[CrossRef](#)]
35. De Alteriis, G.; Violante, C. Catastrophic landslides off Ischia volcanic island (Italy) during prehistory. In *Geohazard in Rocky Coastal Areas*; Violante, C., Ed.; The Geological Society: London, UK, 2009; Volume 322, pp. 73–104. [[CrossRef](#)]
36. Sbrana, A.; Toccaceli, R.M.; Biagio, G.; Cubellis, E.; Faccenna, C.; Fedi, M.; Florio, G.; Fulignati, P.; Giordano, F.; Giudetti, G.; et al. *Geologic Map of Ischia, Scale 1:10.000—Maps and Explanatory Notes*; Campania Region, Sector of Soil Defence, Geothermics and Geotechnics: Naples, Italy, 2011.
37. Sbrana, A.; Marianelli, P.; Pasquini, G. Volcanology of Ischia (Italy). *J. Maps* **2018**, *14*, 494–503. [[CrossRef](#)]
38. Della Seta, M.; Marotta, E.; Orsi, G.; De Vita, S.; Sansivero, F.; Fredi, P. Slope instability induced by volcano-tectonics as an additional source of hazard in active volcanic areas: The case of Ischia island (Italy). *Bull. Volcanol.* **2012**, *74*, 79–106. [[CrossRef](#)]
39. Kilburn, C.R.J.; Carlino, S.; Danesi, S.; Pino, N.A. Potential for rupture before eruption at Campi Flegrei caldera, Southern Italy. *Commun. Earth Environ.* **2023**, *4*, 190. [[CrossRef](#)]
40. De Novellis, V.; Carlino, S.; Castaldo, R.; Tramelli, A.; De Luca, C.; Pino, N.A.; Pepe, S.; Convertito, V.; Zinno, I.; De Martino, P.; et al. The 21 August 2017 Ischia (Italy) earthquake source model inferred from seismological, GPS, and DInSAR measurements. *Geophys. Res. Lett.* **2018**, *45*, 2193–2202. [[CrossRef](#)]
41. Di Fiore, V.; Aiello, G.; D’Argenio, B. Gravity instabilities in the Dohrn Canyon (Bay of Naples, Southern Tyrrhenian Sea): Potential wave and run-up (tsunami) reconstruction from a fossil submarine landslide. *Geol. Carpathica* **2011**, *62*, 55–63. [[CrossRef](#)]
42. Pratson, L.F.; Coakley, B.J. A model for the headward erosion of submarine canyons induced by downslope-eroding sediment flows. *Geol. Soc. Am. Bull.* **1996**, *108*, 225–234. [[CrossRef](#)]
43. Aiello, G.; Caccavale, M. The Coastal Areas of the Bay of Naples: The Sedimentary Dynamics and Geological Evolution of the Naples Canyons. *Geosciences* **2023**, *13*, 226. [[CrossRef](#)]
44. Satow, C.; Watt, S.; Cassidy, M.; Pyle, D.; Deng, Y.N. The Contributions of Marine Sediment Cores to Volcanic Hazard Assessments: Present Examples and Future Perspectives. *Geosciences* **2023**, *13*, 124. [[CrossRef](#)]
45. Brown, R.J.; Orsi, G.; De Vita, S. New insights into Late Pleistocene explosive volcanic activity and caldera formation on Ischia (southern Italy). *Bull. Volcanol.* **2008**, *70*, 583–603. [[CrossRef](#)]
46. de Alteriis, G.; Insinga, D.D.; Morabito, S.; Morra, V.; Chiocci, F.L.; Terrasi, F.; Lubritto, C.; Di Benedetto, C.; Pazzanese, M. Age of submarine debris avalanches and tephrostratigraphy offshore Ischia Island, Tyrrhenian Sea, Italy. *Mar. Geol.* **2010**, *278*, 1–18. [[CrossRef](#)]
47. de Vita, S.; Di Vito, M.A.; Gialanella, C.; Sansivero, F. The impact of the Ischia Porto Tephra eruption (Italy) on the Greek colony of Pithekoussai. *Quat. Int.* **2013**, *303*, 142–152. [[CrossRef](#)]
48. Tomlinson, E.; Albert, P.G.; Wulf, S.; Brown, R.J.; Smith, V.C.; Keller, J.; Orsi, G.; Bourne, A.J.; Menzies, M.A. Age and geochemistry of tephra layers from Ischia, Italy: Constraints from proximal-distal correlations with Lago Grande di Monticchio. *J. Volcanol. Geoth. Res.* **2014**, *287*, 22–39. [[CrossRef](#)]
49. D’Antonio, M.; Arienzo, I.; Brown, R.J.; Petrosino, P.; Pelullo, C.; Giaccio, B. Petrography and Mineral Chemistry of Monte Epomeo Green Tuff, Ischia Island, South Italy: Constraints for Identification of the Y-7 Tephrostratigraphic Marker in Distal Sequences of the Central Mediterranean. *Minerals* **2021**, *11*, 955. [[CrossRef](#)]
50. Primerano, P.; Giordano, G.; Costa, A.; de Vita, S.; Di Vito, M.A. Reconstructing fallout features and dispersal of Cretatio Tephra (Ischia Island, Italy) through field data analysis and numerical modelling: Implications for hazard assessment. *J. Volcanol. Geotherm. Res.* **2021**, *415*, 107248. [[CrossRef](#)]
51. Sacchi, M.; Insinga, D.; Milia, A.; Molisso, F.; Raspini, A.; Torrente, M.M.; Conforti, A. Stratigraphic signature of the Vesuvius 79 AD event off the Sarno prodelta system, Naples Bay. *Mar. Geol.* **2005**, *222–223*, 443–469. [[CrossRef](#)]
52. Insinga, D.D.; Petrosino, P.; Alberico, I.; de Lange, G.J.; Lubritto, C.; Molisso, F.; Sacchi, M.; Sulpizio, R.; Wu, J.; Lirer, F. The Late Holocene tephra record of the central Mediterranean Sea: Mapping occurrences and new potential isochrons for the 4.4–2.0 ka time interval. *J. Quat. Sci.* **2020**, *35*, 213–231. [[CrossRef](#)]
53. Sacchi, M.; Passaro, S.; Molisso, F.; Matano, F.; Steinmann, L.; Spiess, V.; Pepe, F.; Corradino, M.; Caccavale, M.; Tamburrino, S.; et al. The Holocene marine record of unrest, volcanism, and hydrothermal activity of Campi Flegrei and Somma Vesuvius. In *Vesuvius, Campi Flegrei, and Campanian Volcanism*; De Vivo, B., Belkin, H.E., Rolandi, G., Eds.; Elsevier Inc.: Amsterdam, The Netherlands, 2020; pp. 435–469.

54. de Vita, S.; Sansivero, F.; Orsi, G.; Marotta, E.; Piochi, M. Volcanological and structural evolution of the Ischia resurgent caldera (Italy) over the past 10 k.y. In *Stratigraphy and Geology of Volcanic Areas*; GropPELLI, G., Viereck, L., Eds.; GSA Book Series, Special Paper; Geological Society of America: Boulder, CO, USA, 2010; Volume 464, pp. 193–239.
55. Alberico, I.; Lirer, L.; Petrosino, P.; Scandone, R. Volcanic hazard and risk assessment from pyroclastic flows at Ischia Island (southern Italy). *J. Volcanol. Geotherm Res.* **2008**, *171*, 118–136. [[CrossRef](#)]
56. Gurioli, L.; Cioni, R.; Sbrana, A.; Zanella, E. Transport and deposition of pyroclastic density currents over an inhabited area: The deposits of the AD 79 eruption of Vesuvius at Herculaneum (Italy). *Sedimentology* **2002**, *49*, 929–953. [[CrossRef](#)]
57. Cioni, R.; Gurioli, L.; Lanza, R.; Zanella, E. Temperatures of the A.D. 79 pyroclastic density current deposits (Vesuvius, Italy). *J. Geophys. Res.* **2004**, *109*, B02207. [[CrossRef](#)]
58. Gurioli, L.; Zanella, E.; Pareschi, M.T.; Lanza, R. Influences of urban fabric on pyroclastic density currents at Pompeii (Italy) I: Flow direction and deposition. *J. Geophys. Res.* **2007**, *112*, B05213. [[CrossRef](#)]
59. Shea, T.; Gurioli, L.; Houghton, B.F.; Cioni, R.; Cashman, K.V. Column collapse and generation of pyroclastic density currents during the A.D. 79 eruption of Vesuvius: The role of pyroclastic density. *Geology* **2011**, *39*, 695–698. [[CrossRef](#)]
60. Cioni, R.; Tadini, A.; Gurioli, L.; Bertagnini, A.; Mulas, M.; Bevilacqua, A.; Neri, A. Estimating eruptive parameters and related uncertainties for pyroclastic density current deposits: Worked examples from Somma-Vesuvius (Italy). *Bull. Volcanol.* **2020**, *82*, 65. [[CrossRef](#)]
61. Tadini, A.; Bevilacqua, A.; Neri, A.; Cioni, R.; Biagioli, G.; Vitturi, M.; Esposti Ongaro, T. Reproducing pyroclastic density current deposits of the 79 CE eruption of the Somma-Vesuvius volcano using the box-model approach. *Solid Earth* **2021**, *12*, 119–139.
62. Aiello, G. Submarine Stratigraphy of the Eastern Bay of Naples: New Seismo-Stratigraphic Data and Implications for the Somma-Vesuvius and Campi Flegrei Volcanic Activity. *J. Mar. Sci. Eng.* **2022**, *10*, 1520. [[CrossRef](#)]
63. Milia, A.; Molisso, F.; Raspini, A.; Sacchi, M.; Torrente, M.M. Syneruptive features and sedimentary processes associated with pyroclastic currents entering the sea: The AD 79 eruption of Vesuvius, Bay of Naples, Italy. *J. Geol. Soc. Lond.* **2008**, *165*, 839–848. [[CrossRef](#)]
64. Sparks, R.S.J.; Sigurdsson, H.; Carey, S.N. The entrance of pyroclastic flows into the sea, II. Theoretical considerations on subaqueous emplacement and welding. *J. Volcanol. Geoth. Res.* **1980**, *7*, 97–105.
65. Trofimovs, J.; Sparks, R.S.J.; Talling, P.J. Anatomy of a submarine pyroclastic flow and associated turbidity current: July 2003 dome collapse, Soufrière Hills volcano, Montserrat, West Indies. *Sedimentology* **2008**, *55*, 617–634. [[CrossRef](#)]
66. Di Capua, A.; GropPELLI, G. Emplacement of pyroclastic density currents (PDCs) in a deep-sea environment: The Val d’Aveto Formation case (Northern Apennines, Italy). *J. Volcanol. Geoth. Res.* **2016**, *328*, 1–8. [[CrossRef](#)]
67. Clare, M.A.; Yeo, I.A.; Watson, S.; Wysoczanski, R.; Seabrook, S.; Mackay, K.; Hunt, J.E.; Lane, E.; Talling, P.J.; Pope, E.; et al. Fast and destructive density currents created by ocean-entering volcanic eruptions. *Science* **2023**, *381*, 1085–1092. [[CrossRef](#)] [[PubMed](#)]
68. Maeno, F.; Imamura, F. Tsunami generation by a rapid entrance of pyroclastic flow into the sea during the 1883 Krakatau eruption, Indonesia. *J. Geophys. Res.* **2011**, *116*, B09205. [[CrossRef](#)]
69. Alberico, I.; Di Fiore, V.; Iavarone, R.; Petrosino, P.; Piemontese, L.; Tarallo, D.; Punzo, M.; Marsella, E. The Tsunami Vulnerability Assessment of Urban Environments through Freely Available Datasets: The Case Study of Napoli City (Southern Italy). *J. Mar. Sci. Eng.* **2015**, *3*, 981–1005. [[CrossRef](#)]
70. Paris, R.; Ulvrova, M.; Selva, J.; Brizuela, B.; Costa, A.; Grezio, A.; Lorito, S.; Tonini, R. Probabilistic hazard analysis for tsunamis generated by subaqueous volcanic explosions in the Campi Flegrei caldera, Italy. *J. Volcanol. Geotherm. Res.* **2019**, *379*, 106–116. [[CrossRef](#)]
71. Rosi, M.; Levi, S.T.; Pistolesi, M.; Bertagnini, A.; Brunelli, D.; Cannavò, V.; Di Renzoni, A.; Ferranti, F.; Renzulli, A.; Yoon, D. Geoarchaeological Evidence of Middle-Age Tsunamis at Stromboli and Consequences for the Tsunami Hazard in the Southern Tyrrhenian Sea. *Sci. Rep.* **2019**, *9*, 677. [[CrossRef](#)]
72. Maramai, A.; Graziani, L.; Brizuela, B. Italian Tsunami Effects Database (ITED): The First Database of Tsunami Effects Observed Along the Italian Coasts. *Front. Earth Sci.* **2021**, *9*, 596044. [[CrossRef](#)]
73. Tateo, F. Horribile dictu: Environmental catastrophes and writing in the late Middle Ages. In *Le Calamità Ambientali nel Tardo Medioevo Europeo: Realtà, Percezioni, Reazioni, Proceedings of the Atti del XII Convegno del Centro Studi Sulla Civiltà del Tardo Medioevo, San Miniato, Italy, 31 May–2 June 2008*; Centro Studi Sulla Civiltà del Tardo Med; Mattheus, M., Ed.; Firenze University Press: Firenze, Italy, 2010; Volume 12, p. 111. ISBN 978-88-8453-499-6. (In Italian)

Disclaimer/Publisher’s Note: The statements, opinions and data contained in all publications are solely those of the individual author(s) and contributor(s) and not of MDPI and/or the editor(s). MDPI and/or the editor(s) disclaim responsibility for any injury to people or property resulting from any ideas, methods, instructions or products referred to in the content.